

## Resolving the octant of $\theta_{23}$ with T2K and NO $\nu$ A

---

Sanjib Kumar Agarwalla,<sup>a,b</sup> Suprabh Prakash,<sup>c</sup> S. Uma Sankar<sup>c</sup>

<sup>a</sup>*Institute of Physics, Sachivalaya Marg, Sainik School Post, Bhubaneswar 751005, India*

<sup>b</sup>*Instituto de Física Corpuscular, CSIC-Universitat de València,  
Apartado de Correos 22085, E-46071 Valencia, Spain*

<sup>c</sup>*Department of Physics, Indian Institute of Technology Bombay, Mumbai 400076, India*

*E-mail:* [sanjib@iopb.res.in](mailto:sanjib@iopb.res.in), [suprabh@phy.iitb.ac.in](mailto:suprabh@phy.iitb.ac.in), [uma@phy.iitb.ac.in](mailto:uma@phy.iitb.ac.in)

**ABSTRACT:** Preliminary results of MINOS experiment indicate that  $\theta_{23}$  is not maximal. Global fits to world neutrino data suggest two nearly degenerate solutions for  $\theta_{23}$ : one in the lower octant (LO:  $\theta_{23} < 45^\circ$ ) and the other in the higher octant (HO:  $\theta_{23} > 45^\circ$ ).  $\nu_\mu \rightarrow \nu_e$  oscillations in superbeam experiments are sensitive to the octant and are capable of resolving this degeneracy. We study the prospects of this resolution by the current T2K and upcoming NO $\nu$ A experiments. Because of the hierarchy- $\delta_{CP}$  degeneracy and the octant- $\delta_{CP}$  degeneracy, the impact of hierarchy on octant resolution has to be taken into account. As in the case of hierarchy determination, there exist favorable (unfavorable) values of  $\delta_{CP}$  for which octant resolution is easy (challenging). However, for octant resolution the unfavorable  $\delta_{CP}$  values of the neutrino data are favorable for the anti-neutrino data and vice-versa. This is in contrast to the case of hierarchy determination. In this paper, we compute the combined sensitivity of T2K and NO $\nu$ A to resolve the octant ambiguity. If  $\sin^2 \theta_{23} = 0.41$ , then NO $\nu$ A can rule out all the values of  $\theta_{23}$  in HO at  $2\sigma$  C.L., irrespective of the hierarchy and  $\delta_{CP}$ . Addition of T2K data improves the octant sensitivity. If T2K were to have equal neutrino and anti-neutrino runs of 2.5 years each, a  $2\sigma$  resolution of the octant becomes possible provided  $\sin^2 \theta_{23} \leq 0.43$  or  $\geq 0.58$  for any value of  $\delta_{CP}$ .

**KEYWORDS:** Octant of  $\theta_{23}$ , Long-Baseline Experiments: T2K and NO $\nu$ A

---

## Contents

<b>1</b>	<b>Introduction and Motivation</b>	<b>1</b>
<b>2</b>	<b>Present Understanding of the 2-3 mixing angle</b>	<b>3</b>
<b>3</b>	<b>Physics of the octant of <math>\theta_{23}</math></b>	<b>4</b>
<b>4</b>	<b>Event Rates for T2K and NO<math>\nu</math>A</b>	<b>7</b>
<b>5</b>	<b>Results</b>	<b>10</b>
5.1	Allowed regions in test $\sin^2 \theta_{23}$ - true $\delta_{\text{CP}}$ plane	10
5.2	$\Delta\chi^2$ vs. true $\delta_{\text{CP}}$ plots	14
5.3	Octant resolution as function of true $\theta_{23}$	16
<b>6</b>	<b>Summary and Conclusions</b>	<b>17</b>
<b>A</b>	<b>Events vs. <math>\delta_{\text{CP}}</math></b>	<b>18</b>
<b>B</b>	<b>Allowed regions in test <math>\delta_{\text{CP}}</math> - test <math>\sin^2 \theta_{23}</math> plane</b>	<b>20</b>

---

## 1 Introduction and Motivation

Our understanding of the smallest lepton mixing angle  $\theta_{13}$  has improved quite dramatically in last one year or so and finally it has been confirmed to be non-zero with unprecedented confidence by the reactor experiments Daya Bay [1] and RENO [2]. They have found a reasonably large 1-3 mixing

$$\begin{aligned}\sin^2 2\theta_{13}|_{\text{DayaBay}} &= 0.089 \pm 0.010 (\text{stat}) \pm 0.005 (\text{syst}) [3], \text{ and} \\ \sin^2 2\theta_{13}|_{\text{RENO}} &= 0.113 \pm 0.013 (\text{stat}) \pm 0.019 (\text{syst}) [4],\end{aligned}$$

in agreement with the measurements performed earlier by T2K [5, 6], MINOS [7, 8], and Double Chooz [9, 10] experiments. Combined analyses of all the neutrino oscillation data available [11–13] imply a non-zero value of  $\theta_{13}$  at more than  $10\sigma$  and predict a best-fit value of  $\sin^2 \theta_{13} \simeq 0.023$  with a relative  $1\sigma$  precision of 10%. These recent high precision measurements of  $\theta_{13}$  have taken us one step further in validating the standard three flavor oscillation picture of neutrinos on a strong footing [14]. Also, a moderately large value of  $\theta_{13}$  has provided a ‘golden’ opportunity to directly determine the neutrino mass hierarchy<sup>1</sup>

---

<sup>1</sup>Two possibilities are there: it can be either normal (NH) if  $\Delta_{31} \equiv m_3^2 - m_1^2 > 0$ , or inverted (IH) if  $\Delta_{31} < 0$ .

(NMH) using the Earth matter effects, and to unravel the evidence of leptonic CP violation (LCPV)<sup>2</sup> in accelerator based long-baseline neutrino oscillation experiments [15].

Another recent and crucial development is the indication of non-maximal  $\theta_{23}$  by the MINOS accelerator experiment [8]. However, the atmospheric neutrino data, dominated by Super-Kamiokande, still prefers the maximal value of  $\theta_{23}$  [16]. All the three global fits of world neutrino data [11–13] also point to the deviation from maximal mixing for  $\theta_{23}$  *i.e.*  $(0.5 - \sin^2 \theta_{23}) \neq 0$ .

Both these new measurements, non-zero value of  $\theta_{13}$  and non-maximal  $\theta_{23}$ , will provide crucial inputs to the theories of neutrino masses and mixings [17–20]. A number of innovative ideas, such as  $\mu \leftrightarrow \tau$  symmetry [21–29],  $A_4$  flavor symmetry [30–34], and quark-lepton complementarity [35–38] have been invoked to explain the observed pattern of one small and two large mixing angles in the neutrino sector. Measurements of the precise values of  $\theta_{13}$  and  $\theta_{23}$  will reveal the pattern of deviations from these symmetries and will lead to a better understanding of neutrino masses and mixings. In particular, the resolution of  $\theta_{23}$  octant will severely constrain the patterns of symmetry breaking.

In  $\nu_\mu$  survival probability, the dominant term is mainly sensitive to  $\sin^2 2\theta_{23}$ . Now, if  $\sin^2 2\theta_{23}$  differs from 1 as indicated by the recent neutrino data, then we get two solutions for  $\theta_{23}$ : one  $< 45^\circ$ , termed as lower octant (LO) and the other  $> 45^\circ$ , termed as higher octant (HO). In other words, if the quantity  $(0.5 - \sin^2 \theta_{23})$  is positive (negative) then  $\theta_{23}$  belongs to LO (HO). This is known as the octant degeneracy of  $\theta_{23}$  [39] which is a part of the overall eight-fold degeneracy [40, 41], where the other two degeneracies are  $(\theta_{13}, \delta_{\text{CP}})$  intrinsic degeneracy [42] and the (hierarchy,  $\delta_{\text{CP}}$ ) degeneracy [43].

The octant ambiguity of  $\theta_{23}$  is considered to be the most difficult one to deal with among the eight-fold parameter degeneracies. In the past when we had only an upper bound on  $\theta_{13}$ , a possible way of resolving this degeneracy by combining future reactor data with accelerator  $\nu_\mu$  disappearance and  $\nu_e$  appearance measurements was suggested in [44, 45]. Adding the information from the ‘silver’ channel ( $\nu_e \rightarrow \nu_\tau$ ) to the ‘golden’ channel ( $\nu_e \rightarrow \nu_\mu$ ) in the proposed neutrino factory setup is demonstrated to be one of the elegant ways to tackle this degeneracy [46, 47]. The possibility of determining the deviation of  $\theta_{23}$  from maximal mixing and consequently the correct octant of  $\theta_{23}$  in very long-baseline neutrino oscillation experiments and as well as in future atmospheric neutrino experiments has been discussed in [48–56]. One clear message that has been conveyed by all these novel works is that one can achieve a very good sensitivity to the quantity  $|0.5 - \sin^2 \theta_{23}|$  from the conventional beam experiments (MINOS, ICARUS and OPERA), the current generation superbeam experiments (presently running T2K and upcoming NO $\nu$ A), and also from the current (Super-Kamiokande) and future atmospheric data (India-based Neutrino Observatory). But, determining the sign of  $|0.5 - \sin^2 \theta_{23}|$  is deemed to be a very difficult job to pursue and it demands a large value of  $\theta_{13}$ .

Now, in the light of recently discovered moderately large value of  $\theta_{13}$ , it would be quite interesting to study whether the expected appearance data from the ongoing T2K experiment [6, 57] in Japan and the upcoming NO $\nu$ A experiment [58, 59] in the United

---

<sup>2</sup>If the Dirac CP phase,  $\delta_{\text{CP}}$  differs from 0 or  $180^\circ$ .

States can resolve the octant ambiguity of  $\theta_{23}$  or not? In this paper, we address this issue.

The structure of the paper is as follows. We start in section 2 by revisiting our present understanding of the 2-3 mixing angle. Section 3 describes in detail the physics issues related to the octant of  $\theta_{23}$ . We show the event rates for T2K and NO $\nu$ A in section 4. At the end of this section, we also describe the simulation method followed. We present our results in section 5. Finally, in section 6, we summarize and draw our conclusions. Expected events rates in T2K and NO $\nu$ A (both for neutrino and anti-neutrino) as a function of  $\delta_{\text{CP}}$  can be found in Appendix A. Allowed regions in the  $\sin^2 \theta_{23}(\text{test}) - \delta_{\text{CP}}(\text{test})$  plane for the true value of  $\delta_{\text{CP}} = 0$  and all the four combinations of true hierarchy and true octant are shown in Appendix B.

## 2 Present Understanding of the 2-3 mixing angle

Our present knowledge of  $\theta_{23}$  comes from two sources: a) atmospheric neutrinos and b) accelerator neutrinos. In both cases, the muon neutrino disappearance is parametrized in the form of two-flavor survival probability

$$P_{\mu\mu} = 1 - \sin^2 2\theta_{\text{eff}} \sin^2 \left( \frac{\Delta m_{\text{eff}}^2 L}{4E} \right). \quad (2.1)$$

Analysis of the data gives reasonably precise values for the effective two-flavor parameters. Relating these to the three flavor parameters depends on the experimental set up. In the case of atmospheric neutrinos, the path lengths involved vary from 20 km to 13000 km and the energies vary from 200 MeV to a few GeV. This represents a very wide range in  $L/E$ . The approximations valid for some values of  $L/E$  are not valid for others. Therefore, for atmospheric neutrinos, it is not possible to obtain a direct relation between the effective two-flavor parameters and the three-flavor parameters. However, for accelerator neutrinos,  $L$  and  $E$  are chosen so that  $\Delta_{31}L/E \sim 90^\circ$ . Hence,  $\Delta_{21}L/E \ll 1$  ( $\Delta_{21} = m_2^2 - m_1^2$ ) and can be treated as a small perturbation. In this approximation, it was shown that [60–62]

$$\Delta m_{\text{eff}}^2 = \Delta_{31} - (\cos^2 \theta_{12} - \cos \delta_{\text{CP}} \sin \theta_{13} \sin 2\theta_{12} \tan \theta_{23}) \Delta_{21}, \quad (2.2)$$

$$\sin^2 2\theta_{\text{eff}} = 4 \cos^2 \theta_{13} \sin^2 \theta_{23} (1 - \cos^2 \theta_{13} \sin^2 \theta_{23}). \quad (2.3)$$

The mixing angles and phases are defined according to the Particle Data Group convention [63]. The atmospheric neutrino data, dominated by Super-Kamiokande, still prefers the maximal value of  $\sin^2 2\theta_{\text{eff}} = 1$  ( $\geq 0.94$  (90% C.L.)) [16]. But the preliminary results from the MINOS accelerator experiment favor a non-maximal value of  $\sin^2 2\theta_{\text{eff}} = 0.94_{-0.05}^{+0.04}$  [8].

Reference	Forero et.al. [11]	Fogli et.al. [12]	Gonzalez-Garcia et.al. [13]
$\sin^2 \theta_{23}$ (NH)	$0.427^{+0.034}_{-0.027} \oplus 0.613^{+0.022}_{-0.040}$	$0.386^{+0.024}_{-0.021}$	$0.41^{+0.037}_{-0.025} \oplus 0.59^{+0.021}_{-0.022}$
$3\sigma$ range	$0.36 \rightarrow 0.68$	$0.331 \rightarrow 0.637$	$0.34 \rightarrow 0.67$
$\sin^2 \theta_{23}$ (IH)	$0.600^{+0.026}_{-0.031}$	$0.392^{+0.039}_{-0.022}$	
$3\sigma$ range	$0.37 \rightarrow 0.67$	$0.335 \rightarrow 0.663$	

**Table 1:**  $1\sigma$  bounds on  $\sin^2 \theta_{23}$  from the global fits performed in References [11], [12], and [13]. NH and IH stand for normal and inverted hierarchies. The numbers cited from Ref. [13] are those obtained by keeping the reactor fluxes free in the fit and also including the short-baseline reactor data with  $L \lesssim 100$  m, with the mass hierarchy marginalized.

Global fits, using three-flavor oscillations, give information directly on  $\theta_{23}$  rather than  $\theta_{\text{eff}}$ . The best-fit values and ranges of  $\theta_{23}$  from the three recent global fits [11], [12], and [13] are listed in Table 1. A common feature that has emerged from all the three global fits of the world neutrino data is that we now have indication for non-maximal  $\theta_{23}$ . Thus, we have the two degenerate solutions: either  $\theta_{23}$  belongs to the LO ( $\sin^2 \theta_{23} \approx 0.4$ ) or it lies in the HO ( $\sin^2 \theta_{23} \approx 0.6$ ). This degeneracy, in principle, can be broken with the help of  $\nu_\mu \leftrightarrow \nu_e$  oscillation data. The preferred value would depend on the choice of the neutrino mass hierarchy. However, as can be seen from Table 1, the fits of reference [11] do not agree on which value should be preferred, even when the mass hierarchy is fixed to be NH. In [12], LO is preferred over HO for both NH and IH. Reference [13] marginalizes over the mass hierarchy, so the degeneracy remains. The global best-fits in references [11, 13] do not observe any sensitivity to the octant of  $\theta_{23}$  unless they add the atmospheric neutrino data. But, in [12], they do find a preference for LO even without adding the atmospheric data. In this paper, we take the best-fit value of  $\sin^2 \theta_{23}$  in the lower octant (LO) to be 0.41 while that in the higher octant (HO) to be 0.59 [13].

### 3 Physics of the octant of $\theta_{23}$

In a long-baseline experiment,  $\nu_\mu$  charged current (CC) events are the most copious. These experiments can measure  $\nu_\mu \rightarrow \nu_\mu$  survival probability,  $P_{\mu\mu}$ , as a function of energy. The reconstruction of the minimum of  $P_{\mu\mu}$  leads to precise values for  $|\Delta m_{\text{eff}}^2|$  and  $\sin^2 2\theta_{\text{eff}}$  [8, 60–62]. Therefore, we get two degenerate best-fit values for  $\sin^2 \theta_{23}$ , one in LO and the other in HO, with small allowed regions around them. The  $P_{\mu\mu}$  expression has subleading terms which are sensitive to octant [64]. But, these are suppressed by the small parameter  $\alpha = \Delta_{21}/\Delta_{31}$  and their biggest impact occurs for energies where  $P_{\mu\mu}$  is very small. So, the overall octant sensitivity of  $P_{\mu\mu}$  is negligible. However,  $P_{\mu\mu}$  gives a precise measurement of  $\sin^2 2\theta_{\text{eff}}$  which in turn gives precise allowed regions for  $\sin^2 \theta_{23}$  in the two octants.

In the presence of matter, the  $\nu_\mu \rightarrow \nu_e$  oscillation probability, expanded perturbatively in  $\alpha$  and  $\theta_{13}$ , can be written as [64–66]

$$P_{\mu e} = \beta_1 \sin^2 \theta_{23} + \beta_2 \cos(\hat{\Delta} + \delta_{\text{CP}}) + \beta_3 \cos^2 \theta_{23}. \quad (3.1)$$

In the above equation,  $P_{\mu e}$  is written in a way to highlight the octant and  $\delta_{\text{CP}}$  dependent terms. Here

$$\begin{aligned}\beta_1 &= \sin^2 2\theta_{13} \frac{\sin^2 \hat{\Delta}(1 - \hat{A})}{(1 - \hat{A})^2}, \\ \beta_2 &= \alpha \cos \theta_{13} \sin 2\theta_{12} \sin 2\theta_{13} \sin 2\theta_{23} \frac{\sin \hat{\Delta} \hat{A} \sin \hat{\Delta}(1 - \hat{A})}{\hat{A} (1 - \hat{A})}, \\ \beta_3 &= \alpha^2 \sin^2 2\theta_{12} \cos^2 \theta_{13} \frac{\sin^2 \hat{\Delta} \hat{A}}{\hat{A}^2},\end{aligned}\quad (3.2)$$

with  $\hat{\Delta} = \Delta_{31}L/4E$ ,  $\hat{A} = A/\Delta_{31}$ .  $A$  is the Wolfenstein matter term [67] and is given by  $A(\text{eV}^2) = 0.76 \times 10^{-4} \rho (\text{g/cc})E(\text{GeV})$ .  $\rho$  is the density of matter in the Earth. For NO $\nu$ A and T2K, this is set equal to the density in the crust of 2.8 g/cc.

For normal hierarchy (NH),  $\Delta_{31}$  is positive and for inverted hierarchy (IH), it is negative. The matter term  $A$  is positive for neutrinos and is negative for anti-neutrinos. Hence, in neutrino oscillation probability,  $\hat{A}$  is positive for NH and is negative for IH; vice-versa for anti-neutrinos. Moreover, sign of  $\delta_{\text{CP}}$  is reversed for anti-neutrinos. The left (right) panel of figure 1 shows  $P_{\mu e}$  vs.  $E_\nu$  ( $P_{\bar{\mu}e}$  vs.  $E_{\bar{\nu}}$ ) for all possible values of  $\delta_{\text{CP}}$  and for the two values of  $\sin^2 \theta_{23}$ , assuming NH to be the true hierarchy. These plots are for the experiment NO $\nu$ A .

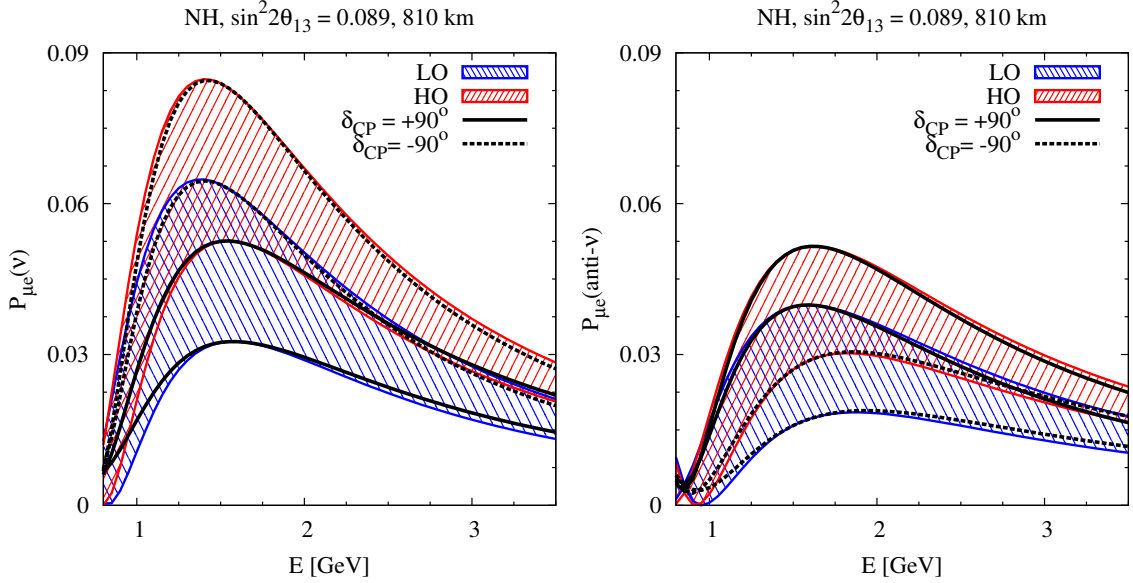


**Figure 1:**  $P_{\mu e}$  as a function of neutrino energy. The left panel (right panel) is for  $\nu$  ( $\bar{\nu}$ ). Here, the bands correspond to different values of  $\delta_{\text{CP}}$  from  $-180^\circ$  to  $180^\circ$ . These plots are for NO $\nu$ A ( $L=810$  km),  $\sin^2 2\theta_{13} = 0.089$  and NH. For LO (HO),  $\sin^2 \theta_{23} = 0.41$  ( $0.59$ ).

As can be seen from the left panel of figure 1, for neutrino data, the two octant bands overlap for some values of  $\delta_{\text{CP}}$  and are distinct for other values. The combinations of octant and  $\delta_{\text{CP}}$  which lie farthest from overlap will be favorable combinations for octant

determination. For example, LO and  $\delta_{\text{CP}}$  of  $90^\circ$  and HO and  $\delta_{\text{CP}}$  of  $-90^\circ$  form the favorable combinations. For the combinations with overlap, HO and  $\delta_{\text{CP}}$  of  $90^\circ$  and LO and  $\delta_{\text{CP}}$  of  $-90^\circ$ , it is impossible to determine octant using neutrino data alone. However, as we see from the right panel, these unfavorable combinations for neutrino case are the favorable ones for the  $\bar{\nu}$  case. Thus, a combination of neutrino and anti-neutrino data will have a better capability to determine octant compared to neutrino data alone. This is in contrast to the hierarchy- $\delta_{\text{CP}}$  degeneracy, where for a given hierarchy, the favorable  $\delta_{\text{CP}}$  region is the same for both  $\nu$  and  $\bar{\nu}$ . Thus, we are led to the conclusion that a balanced neutrino and anti-neutrino data is imperative for resolving the octant for all values of  $\delta_{\text{CP}}$ .

Let us do a small, quantitative analysis of the octant- $\delta_{\text{CP}}$  degeneracy of  $P_{\mu e}$ . A similar analysis for hierarchy- $\delta_{\text{CP}}$  degeneracy was done in [68]. For simplicity, here we keep the hierarchy fixed. Increase in  $\theta_{23}$  increases  $P_{\mu e}$ . While a change in  $\delta_{\text{CP}}$  can increase or decrease  $P_{\mu e}$ . For different  $\delta_{\text{CP}}^{\text{LO}}$  and  $\delta_{\text{CP}}^{\text{HO}}$ ,  $P_{\mu e}(\text{LO}, \delta_{\text{CP}}^{\text{LO}})$  may be very close to  $P_{\mu e}(\text{HO}, \delta_{\text{CP}}^{\text{HO}})$ . For the degenerate case,  $P_{\mu e}(\text{LO}, \delta_{\text{CP}}^{\text{LO}}) = P_{\mu e}(\text{HO}, \delta_{\text{CP}}^{\text{HO}})$ , leading to

$$\cos(\hat{\Delta} + \delta_{\text{CP}}^{\text{LO}}) - \cos(\hat{\Delta} + \delta_{\text{CP}}^{\text{HO}}) = \frac{\beta_1 - \beta_3}{\beta_2} (\sin^2 \theta_{23}^{\text{HO}} - \sin^2 \theta_{23}^{\text{LO}}). \quad (3.3)$$

For the  $\text{NO}\nu\text{A}$  baseline  $L = 810$  km and energy of peak flux  $E = 2$  GeV, we get for NH and  $\nu$

$$\cos(\hat{\Delta} + \delta_{\text{CP}}^{\text{LO}}) - \cos(\hat{\Delta} + \delta_{\text{CP}}^{\text{HO}}) = 1.7. \quad (3.4)$$

The above equation will have solutions only if

$$\begin{aligned} 0.7 &\leq \cos(\hat{\Delta} + \delta_{\text{CP}}^{\text{LO}}) \leq 1.0, \\ -1.0 &\leq \cos(\hat{\Delta} + \delta_{\text{CP}}^{\text{HO}}) \leq -0.7. \end{aligned} \quad (3.5)$$

From this, we get their ranges to be:

$$\begin{aligned} -116^\circ &\leq \delta_{\text{CP}}^{\text{LO}} \leq -26^\circ, \\ 64^\circ &\leq \delta_{\text{CP}}^{\text{HO}} \leq 161^\circ. \end{aligned} \quad (3.6)$$

Thus, we find that for NH and  $\nu$  of energy 2 GeV,  $P_{\mu e}(\text{LO}, -116^\circ \leq \delta_{\text{CP}} \leq -26^\circ)$  is degenerate with  $P_{\mu e}(\text{HO}, 64^\circ \leq \delta_{\text{CP}} \leq 161^\circ)$ . A similar analysis can be done for T2K baseline of  $L = 295$  km and energy of peak flux  $E = 0.6$  GeV. The overlap regions in the  $\delta_{\text{CP}}$  range are essentially the same as above because the values of  $\hat{\Delta}$  and those of  $(\beta_1 - \beta_3)/\beta_2$  are nearly the same for the two experiments. This is to be contrasted with the hierarchy discrimination, where the overlap range for  $\text{NO}\nu\text{A}$  is very different from that of T2K because of widely different matter effects [68, 69].

In figure 2, we show the values of  $\delta_{\text{CP}}$ , which lie in the overlapping region, as a function of energy, for the combinations LO-NH and HO-NH. For the experiment  $\text{NO}\nu\text{A}$ , most of the signal events come from the range 1.5 - 2.5 GeV. Hence, we consider only this energy range in the figure. The blue-dotted (red-crossed) shaded region shows those values of  $\delta_{\text{CP}}$ , for which there is an overlap between  $P_{\mu e}^{\text{LO}}$  and  $P_{\mu e}^{\text{HO}}$ , for  $\nu$  ( $\bar{\nu}$ ) data. These plots show the degenerate octant- $\delta_{\text{CP}}$  values in the relevant energy range and help explain the  $\delta_{\text{CP}}$  dependence seen in octant sensitivity.



The values of  $\delta_{\text{CP}}$  which lie farthest from any of the overlap regions will be the most favored ones. Those  $\delta_{\text{CP}}$  values which lie in one of the overlap region (i.e. either in  $\nu$  or  $\bar{\nu}$ ) but are far from the other overlap region will also be favored (though to a lesser extent than the previous values) if balanced  $\nu$  and  $\bar{\nu}$  runs are taken. The regions of  $\delta_{\text{CP}}$  which are common or very close to both overlap regions will be the most unfavored ones. We find that  $\delta_{\text{CP}} \sim 0$  is the most unfavored for LO-NH and HO-IH whereas  $\delta_{\text{CP}} \sim 180^\circ$  is the most unfavored for HO-NH and LO-IH. This pattern is observed in the results in subsection 5.1.

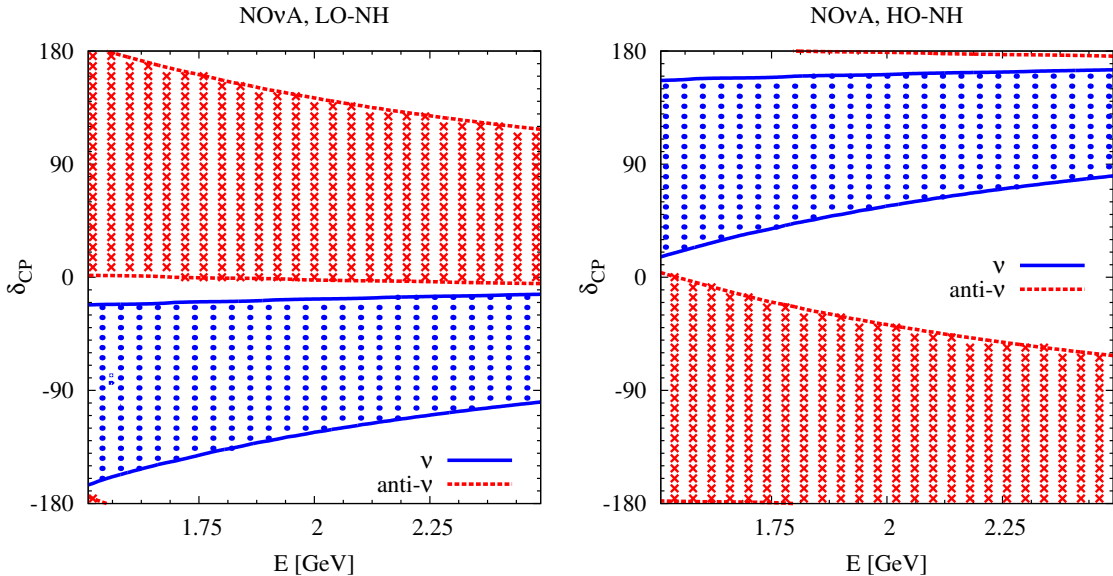


**Figure 2:** Plots showing octant- $\delta_{\text{CP}}$  degeneracy in  $P_{\mu e}$  as a function of neutrino energy. The left (right) panel is for LO (HO). The blue-dotted (red-crossed) regions are for  $\nu$  ( $\bar{\nu}$ ). For a given  $E_\nu$  ( $E_{\bar{\nu}}$ ),  $P_{\mu e}$ [ LO, vertical blue-dotted (red-crossed)  $\delta_{\text{CP}}$  region in the left panel ] values are degenerate with  $P_{\mu e}$ [ HO, vertical blue-dotted (red-crossed)  $\delta_{\text{CP}}$  region in the right panel ] values. The exact degenerate octant- $\delta_{\text{CP}}$  values can be found out using equation 3.4. As an example, for  $E_\nu$  of 2 GeV,  $P_{\mu e}(\text{LO}, \delta_{\text{CP}} = -90^\circ)$  is degenerate with  $P_{\mu e}(\text{HO}, \delta_{\text{CP}} \approx 66^\circ)$ . These plots are for NO $\nu$ A (L=810 km),  $\sin^2 2\theta_{13} = 0.089$  and NH. For LO (HO),  $\sin^2 \theta_{23} = 0.41$  (0.59).

#### 4 Event Rates for T2K and NO $\nu$ A

In this paper, we simulate the data for the two *off-axis* superbeam experiments: T2K and NO $\nu$ A using GLoBES [70, 71]. In the T2K experiment, a  $\nu_\mu$  beam from J-PARC is directed towards Super-Kamiokande detector, 295 km away. The flux peaks sharply at 0.6 GeV, close to the first oscillation maximum in  $P(\nu_\mu \rightarrow \nu_e)$ . The experiment is scheduled to run for 5 years in the neutrino mode only. The details of T2K experiment are given in [57]. The information regarding signal efficiencies and backgrounds are taken from [72, 73]. NO $\nu$ A is a 14 kT totally active scintillator detector located at Ash River; a distance of 810 km from Fermilab. The flux peaks at 2 GeV, again close to the first oscillation maximum in  $P(\nu_\mu \rightarrow \nu_e)$ . This experiment is scheduled to have three years run in neutrino mode first



and then later, three years run in anti-neutrino mode as well. The details of the experiment are given in [74]. In light of the recent measurement of large  $\theta_{13}$ , NO $\nu$ A has reoptimized their signal and background acceptances. In our calculations, we use these reoptimized values, the details of which are given in [59, 75].

In our simulations, we have used the following input values for neutrino oscillation parameters [8, 13].

$$\begin{aligned} |\Delta m_{\text{eff}}^2| &= 2.4 \times 10^{-3} \text{ eV}^2 \\ \Delta_{21} &= 7.5 \times 10^{-5} \text{ eV}^2, \quad \sin^2 \theta_{12} = 0.3 \\ \sin^2 2\theta_{13} &= 0.089 \end{aligned}$$

The value of  $\Delta_{31}$  is calculated separately for NH and for IH using equation 2.2 where  $\Delta m_{\text{eff}}^2$  is taken to be +ve for NH and -ve for IH. The uncertainties in the above parameters are taken to be  $\sigma(|\Delta m_{\text{eff}}^2|) = 4\%$  [8] and  $\sigma(\sin^2 2\theta_{13}) = 5\%$  [76]. The solar parameters ( $\Delta_{21}$  and  $\sin^2 \theta_{12}$ ) and the Earth matter density in the calculation of matter term are held fixed throughout the calculation.

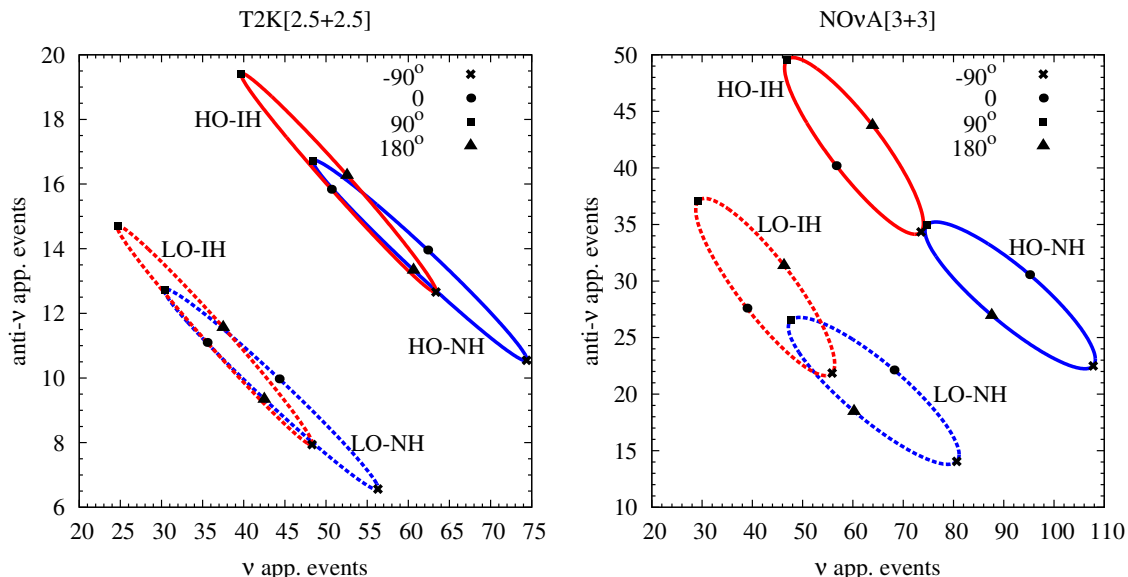


**Figure 3:**  $\nu$  and  $\bar{\nu}$  appearance events for all possible combinations of hierarchy, octant and  $\delta_{\text{CP}}$ . The left (right) panel is for T2K (NO $\nu$ A). Here  $\sin^2 2\theta_{13} = 0.089$ . For LO (HO),  $\sin^2 \theta_{23} = 0.41$  (0.59). Note that for T2K, equal  $\nu$  and  $\bar{\nu}$  runs of 2.5 years each has been assumed. The variation of  $\nu$  and  $\bar{\nu}$  appearance events with  $\delta_{\text{CP}}$  is shown in appendix A for both T2K and NO $\nu$ A .

In figure 3, we plot  $\nu$  events vs.  $\bar{\nu}$  events for various octant-hierarchy combinations. In each case, with varying values of  $\delta_{\text{CP}}$ , the plot becomes an ellipse. The left panel shows these ellipses for T2K whereas the right panel shows the same for NO $\nu$ A . Here, we assumed that T2K will have equal  $\nu$  and  $\bar{\nu}$  runs of 2.5 years each. In the right panel, we see that the ellipses for the two hierarchies overlap whereas the ellipses of LO are well separated from those of HO. Hence, we can expect that NO $\nu$ A will have better octant resolution

capability than hierarchy discrimination. This situation is even more dramatic in the left panel where there is large overlap between the two hierarchies but clear separation between the octants. Thus, it is very likely that  $\bar{\nu}$  data from T2K may play an important role in the determination of octant.

We illustrate the octant determination capability of  $\text{NO}\nu A$  by considering some special points in the right panel. The features that we emphasize here can also be discerned from figure 2.

- LO-NH,  $\delta_{\text{CP}} = 0^\circ$ : The coordinates of this point in the  $\nu$ - $\bar{\nu}$  event plane are (68,22). No point on the HO-NH ellipse has these coordinates but there exist a number of points with coordinates close to these. Therefore, the wrong octant is difficult to rule out for this point.
- LO-NH,  $\delta_{\text{CP}} = 90^\circ$ : The coordinates of this point in the  $\nu$ - $\bar{\nu}$  event plane are (48,27). The  $\nu$  events are much lower than those of all points on the HO-NH ellipse but there is degeneracy in the  $\bar{\nu}$  events. Hence, ruling out the wrong octant should be possible for this point.
- LO-NH,  $\delta_{\text{CP}} = 180^\circ$ : The coordinates of this point in the  $\nu$ - $\bar{\nu}$  event plane are (60,18). Both  $\nu$  and  $\bar{\nu}$  events are much lower than the corresponding events of any point on the HO-NH ellipse. Thus, ruling out the wrong octant will be the easiest for this point.
- LO-NH,  $\delta_{\text{CP}} = -90^\circ$ : An argument similar to the case  $\delta_{\text{CP}} = 90^\circ$  can be made, except that the  $\nu$  events have degeneracy between octants, but the  $\bar{\nu}$  events for this point are much below those of any point on the HO-NH ellipse.

Similar arguments can be made for other octant-hierarchy combinations with the exception that the most favorable and most unfavorable  $\delta_{\text{CP}}$  values will differ.

We see that for the given choices of best-fit value of  $\sin^2 \theta_{23}$ ,  $\text{NO}\nu A$  has very good sensitivity to octant resolution due to balanced  $\nu$  and  $\bar{\nu}$  runs. Because the favorable and unfavorable values of  $\delta_{\text{CP}}$  (pertaining to octant resolution) are different for  $\nu$  and  $\bar{\nu}$ , no  $\delta_{\text{CP}}$  value is absolutely unfavorable if balanced  $\nu$  and  $\bar{\nu}$  runs are taken. Therefore, a single experiment on its own, can have very good sensitivity as illustrated in figure 3. This is in stark contrast to the case of hierarchy, where we saw that having data from two experiments with widely different baselines is a necessity because the favorable and unfavorable combinations turned out to be the same for  $\nu$  and  $\bar{\nu}$ .

Before discussing our results, we briefly describe the numerical procedure adopted. We calculate  $\Delta\chi^2$  using the default definition in GLoBES which is Poissonian. We minimize this  $\Delta\chi^2$  to compute the octant resolution capability. For a given octant-hierarchy combination and a true value of  $\delta_{\text{CP}}$ , we compute the events spectra and label it *data*. Then we compute the theoretical events spectra where the octant is chosen to be the wrong one and the neutrino parameters are randomly chosen within their allowed  $3\sigma$  ranges. We then calculate the  $\Delta\chi^2$  between the data and the theoretical spectra. This calculation uses the  $\Delta\chi^2$  defined in GLoBES, which is valid for a Poissonian distribution. We add a  $\Delta\chi^2$

coming from gaussian priors on  $|\Delta m_{\text{eff}}^2|$  and on  $\sin^2 2\theta_{13}$ . The systematic uncertainties are included using the method of pulls. If the  $\Delta\chi_{\text{min}}^2 \geq 4$ , then we can say that the wrong octant is ruled out at  $2\sigma$  for the given combination and the given true value of  $\delta_{\text{CP}}$ . This calculation is repeated for all true values of  $\delta_{\text{CP}}$  and for all combinations. If the  $\Delta\chi_{\text{min}}^2 \geq 4$  in each case then the wrong octant can be ruled out independently of true  $\delta_{\text{CP}}$ , hierarchy and octant.

## 5 Results

In this section, through various plots, we show the sensitivity of T2K and NO $\nu$ A to the octant of  $\theta_{23}$ .

### 5.1 Allowed regions in test $\sin^2 \theta_{23}$ - true $\delta_{\text{CP}}$ plane

In figures 4-7, we have plotted the values of test  $\sin^2 \theta_{23}$  allowed by T2K and NO $\nu$ A data as a function of true  $\delta_{\text{CP}}$  for each of the four combinations of octant and hierarchy. In our calculations, we do not assume a prior knowledge of hierarchy and hence consider both the possibilities for test hierarchy. Octant can be determined only if the wrong octant values are ruled out for both possibilities.

In this analysis, we have included the data from both the disappearance channel  $P_{\mu\mu}$  and the appearance channel  $P_{\mu e}$ . We varied  $\sin^2 \theta_{23}$  within its  $3\sigma$  range: [0.34, 0.67] allowed by the current global fits. Here, we are constraining  $\sin^2 \theta_{23}$  only and are marginalizing over  $\delta_{\text{CP}}$  and hence take the  $2\sigma$  limit relevant for 1 d.o.f. The contours in these figures are defined by  $\Delta\chi^2 \leq 4$ . *The disappearance channel gives a precise measurement of  $\sin^2 2\theta_{\text{eff}}$  which leads to two narrow,  $\delta_{\text{CP}}$ -independent, allowed  $\sin^2 \theta_{23}$  bands, one in each octant. The appearance channel, because of its large octant sensitivity, discriminates against the wrong octant band.* If the statistics are large enough, the wrong octant can be ruled out.

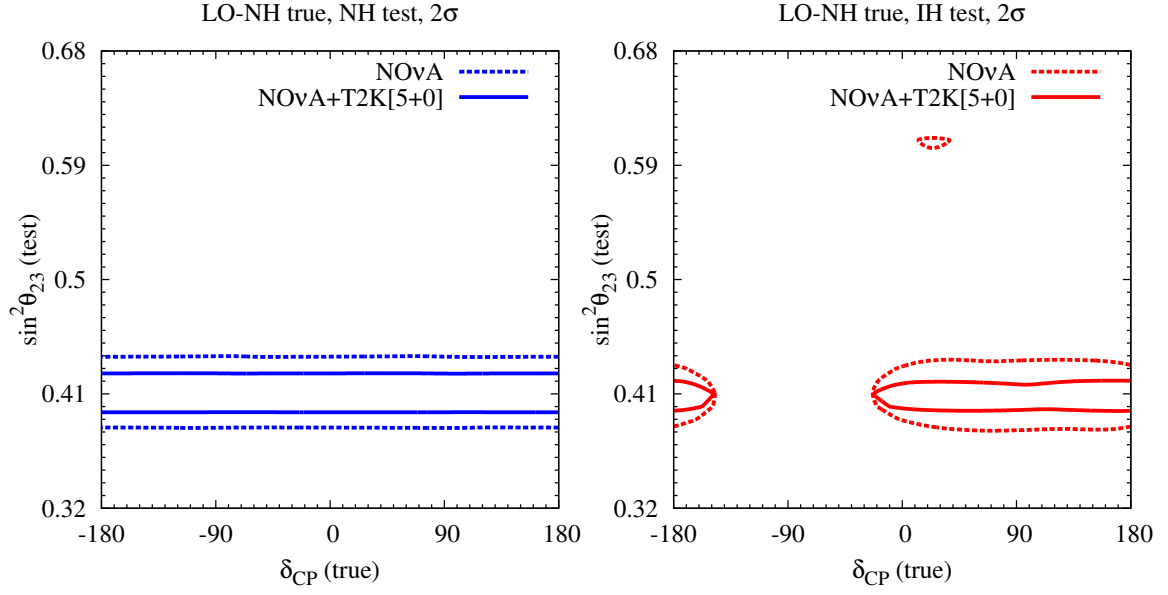


**Figure 4:** Allowed values of test  $\sin^2\theta_{23}$  at  $2\sigma$  (1 d.o.f.) C.L. as a function of true  $\delta_{CP}$ . LO-NH is assumed to be the true octant-hierarchy combination. The left (right) panel corresponds to NH (IH) being the test hierarchy.

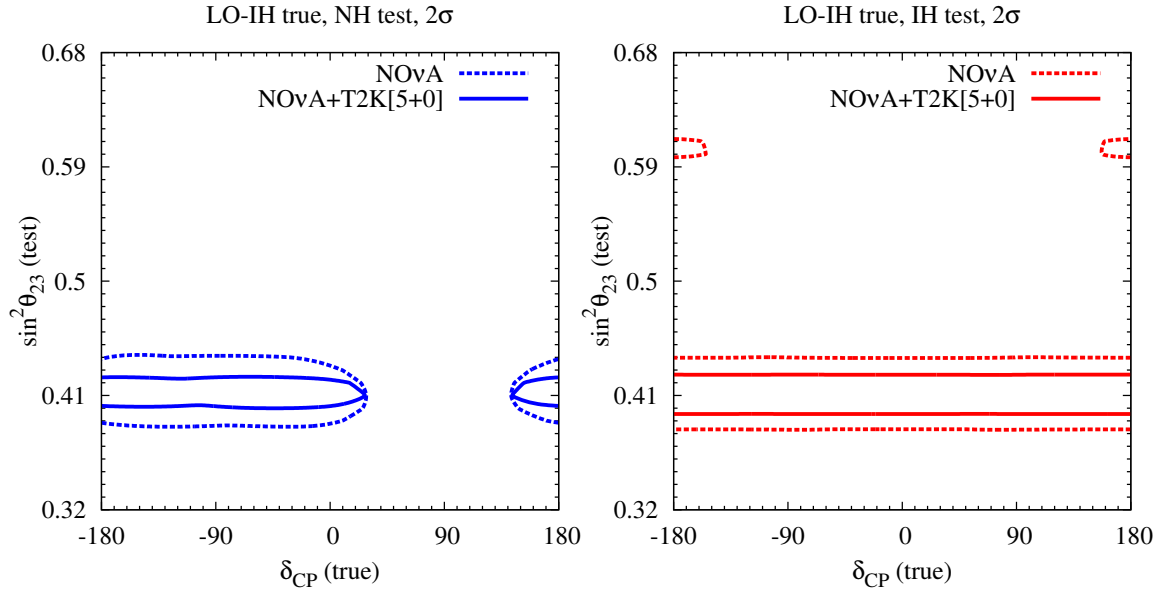


**Figure 5:** Allowed values of test  $\sin^2\theta_{23}$  at  $2\sigma$  (1 d.o.f.) C.L. as a function of true  $\delta_{CP}$ . LO-IH is assumed to be the true octant-hierarchy combination. The left (right) panel corresponds to NH (IH) being the test hierarchy.

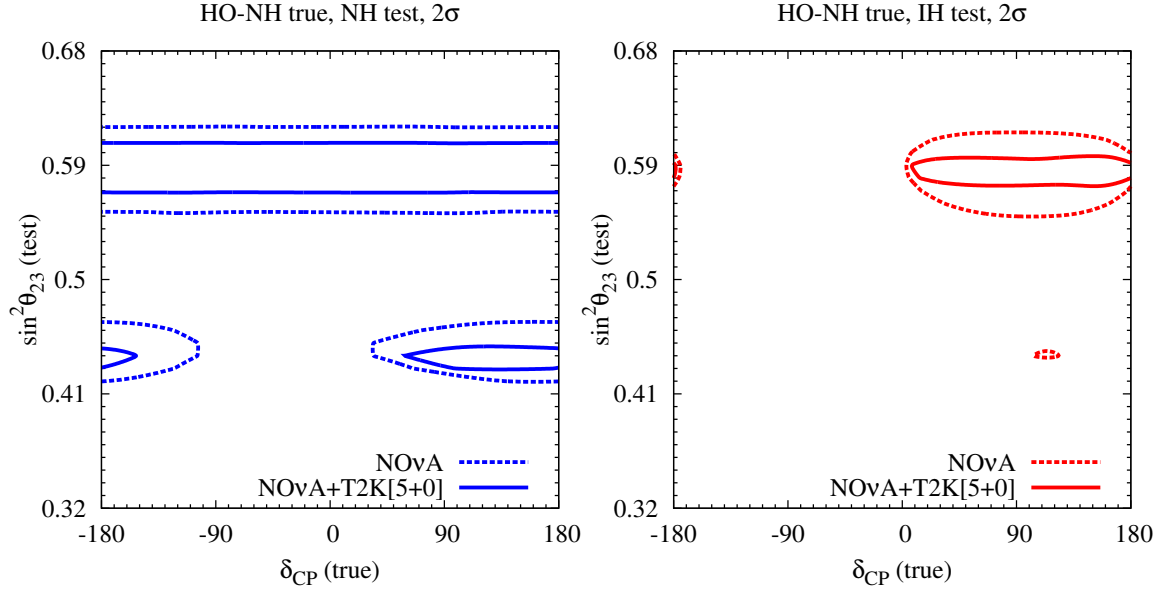


**Figure 6:** Allowed values of test  $\sin^2 \theta_{23}$  at  $2\sigma$  (1 d.o.f. ) C.L. as a function of true  $\delta_{\text{CP}}$ . HO-NH is assumed to be the true octant-hierarchy combination. The left (right) panel corresponds to NH (IH) being the test hierarchy.

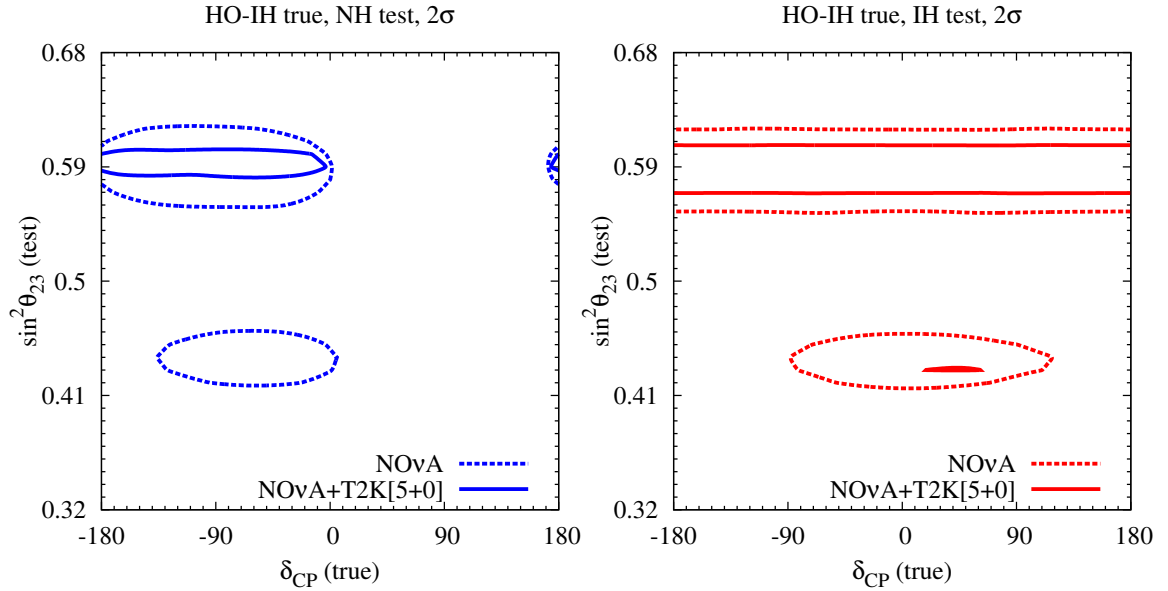


**Figure 7:** Allowed values of test  $\sin^2 \theta_{23}$  at  $2\sigma$  (1 d.o.f. ) C.L. as a function of true  $\delta_{\text{CP}}$ . HO-IH is assumed to be the true octant-hierarchy combination. The left (right) panel corresponds to NH (IH) being the test hierarchy.

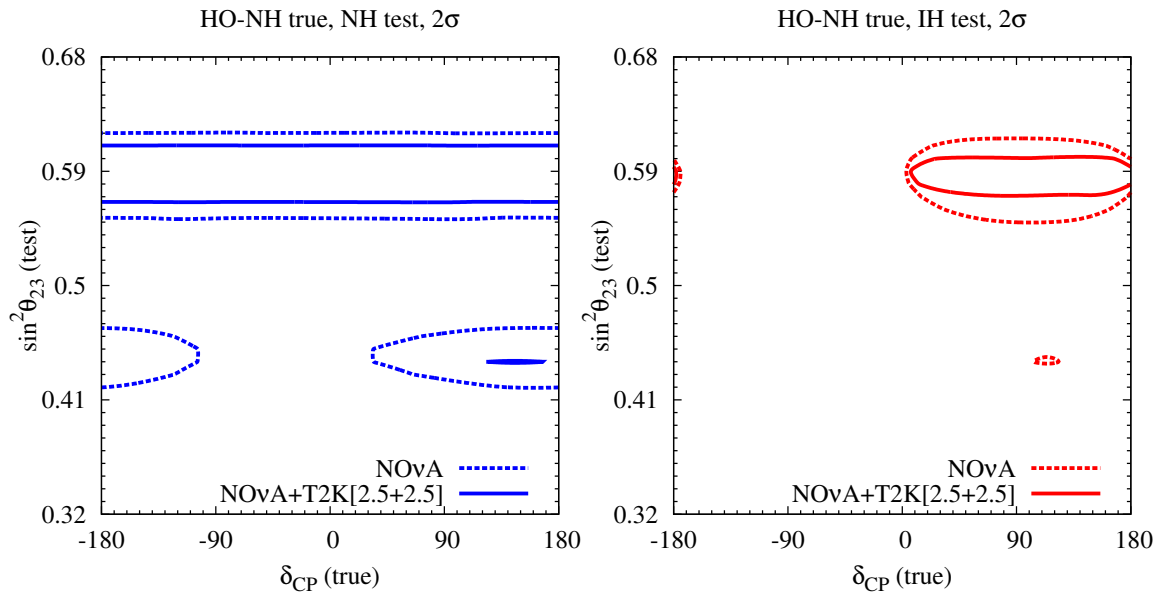


**Figure 8:** Allowed values of test  $\sin^2 \theta_{23}$  at  $2\sigma$  (1 d.o.f.) C.L. as a function of true  $\delta_{\text{CP}}$ . HO-NH is assumed to be the true octant-hierarchy combination. The left (right) panel corresponds to NH (IH) being the test hierarchy. Note that for T2K, equal  $\nu$  and  $\bar{\nu}$  runs of 2.5 years each has been assumed.

From figures 4 and 5, we note that the combined data of T2K and NO $\nu$ A can rule out HO if LO is the true octant. This holds for both NH and IH. However, if HO is the true octant, then LO can not be ruled out for a reasonably large fraction of true  $\delta_{\text{CP}}$ .

As argued in section 3, the favorable and unfavorable regions are very different for neutrinos and anti-neutrinos. Hence, we explored if an improvement in the octant determination can be achieved if T2K has equal neutrino and anti-neutrino runs of 2.5 years each<sup>3</sup>. As expected, in the two cases of LO-NH and LO-IH, a  $(2.5\nu + 2.5\bar{\nu})$  runs in T2K is also effective in ruling out the wrong octant at  $2\sigma$ . Hence, we have not displayed the corresponding figures. But, for the two cases HO-NH and HO-IH, the balanced  $\nu$  and  $\bar{\nu}$  runs are more effective than the  $(5\nu)$  run. This is shown in figures 8 and 9. In the left panel of figure 8, there is a very small sliver of allowed  $\sin^2 \theta_{23}$  in the wrong octant for true  $\delta_{\text{CP}}$  in the range  $[130^\circ, 160^\circ]$ . But, the  $\Delta\chi^2$  for this sliver is very close to 4. Hence, this wrong octant region can be effectively discriminated against, leading to a determination of the octant of  $\theta_{23}$  for any true value of  $\delta_{\text{CP}}$ .

The above set of figures also give the precision on  $\sin^2 \theta_{23}$  that one can obtain. This precision is the result of the precise measurement of  $\sin^2 2\theta_{23}$  from the disappearance channel. From figures 4 and 5, we get  $\delta(\sin^2 \theta_{23}) = 0.015$  if LO is the true octant. From figures 6 and 7, we see that a 5 year  $\nu$  run of T2K combined with NO $\nu$ A gives  $\delta(\sin^2 \theta_{23}) = 0.02$  if HO is the true octant. When the T2K run is changed to  $(2.5\nu + 2.5\bar{\nu})$ , the precision in

<sup>3</sup>In GLoBES, the background events for T2K are given for a 5 year  $\nu$  run taken from [73]. We have taken care to do appropriate scaling of these events in computing for  $(2.5\nu + 2.5\bar{\nu})$  runs.

$\sin^2 \theta_{23}$  becomes slightly worse because of the loss of statistics caused by  $\bar{\nu}$  run as seen in figures 8 and 9.

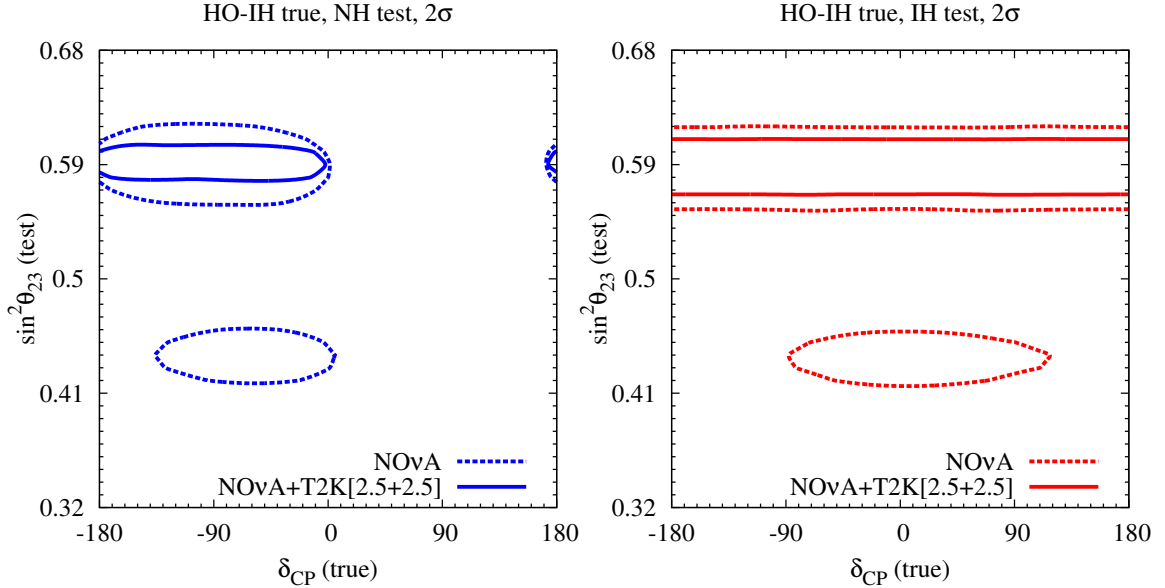


**Figure 9:** Allowed values of test  $\sin^2 \theta_{23}$  at  $2\sigma$  (1 d.o.f. ) C.L. as a function of true  $\delta_{CP}$ . HO-IH is assumed to be the true octant-hierarchy combination. The left (right) panel corresponds to NH (IH) being the test hierarchy. Note that for T2K, equal  $\nu$  and  $\bar{\nu}$  runs of 2.5 years each has been assumed.

## 5.2 $\Delta\chi^2$ vs. true $\delta_{CP}$ plots

In this section, we study the behavior of  $\Delta\chi^2$  between the true and the wrong octants as a function of true  $\delta_{CP}$ . Here, the  $\Delta\chi^2$  is computed in the following way. First, we fix the true value of  $\delta_{CP}$ . We take  $\sin^2 \theta_{23}$  to be its best-fit value in the true octant: 0.41 for LO and 0.59 for HO. If the LO (HO) is the true octant, the test values of  $\sin^2 \theta_{23}$  in the HO (LO) are varied within the range  $[0.5, 0.63]$  ( $[0.36, 0.5]$ ), where 0.63 (0.36) is the  $2\sigma$  upper (lower) limit of the allowed range of  $\sin^2 \theta_{23}$ . The  $\Delta\chi^2$  is computed between the spectra with the best-fit  $\sin^2 \theta_{23}$  of the true octant and that with various test values in the wrong octant and is marginalized over other neutrino parameters, especially the hierarchy,  $\sin^2 2\theta_{13}$  and  $\delta_{CP}$ . Figures 10 and 11 show the minimum of this  $\Delta\chi^2$  vs. the true value of  $\delta_{CP}$ .

From figure 10, we see that the  $\text{NO}\nu\text{A}$  data by itself can almost rule out the wrong octant at  $2\sigma$ , if LO is the true octant. We see that the  $\Delta\chi^2$  dips just below 4 for true  $\delta_{CP} \sim 0(180^\circ)$  if the true hierarchy is NH (IH). But, as argued earlier, this small allowed region can be effectively discriminated because of the relatively large  $\Delta\chi^2$ . If HO is the true octant, then  $\text{NO}\nu\text{A}$  data is not sufficient to rule out the wrong octant as seen in figure 11. In fact, the wrong octant can be ruled out only for about half of the true  $\delta_{CP}$  values. As illustrated in figures 10 and 11, addition of T2K data improves the octant determination ability significantly.



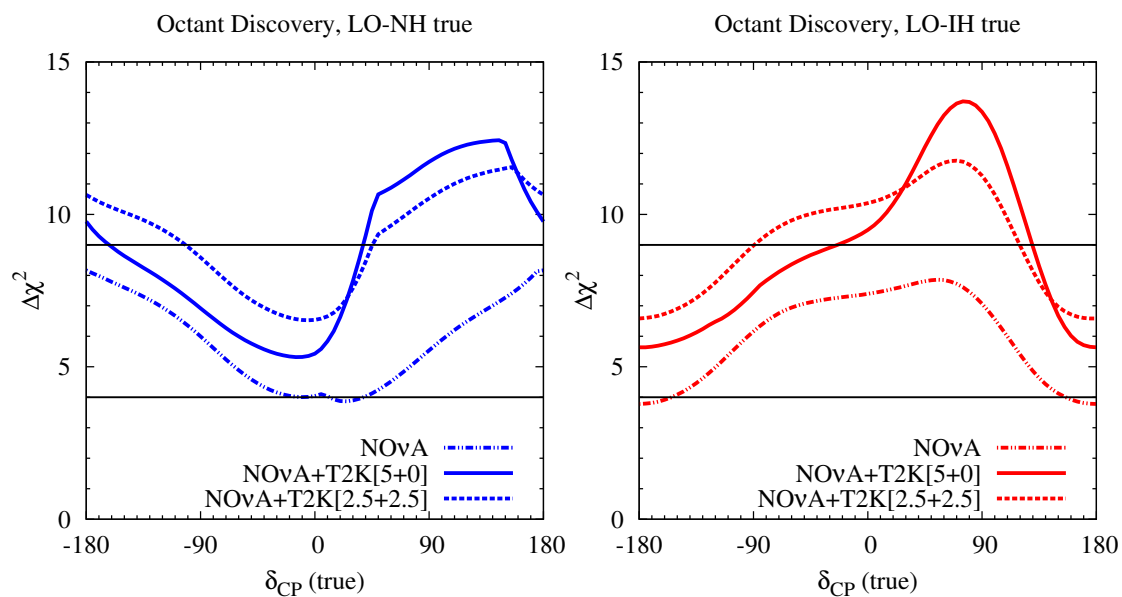


**Figure 10:** Octant resolving capability as a function of true  $\delta_{\text{CP}}$  for various set-ups . In these plots, LO is assumed to be the true octant. The left (right) panel corresponds to NH (IH) being the true hierarchy.

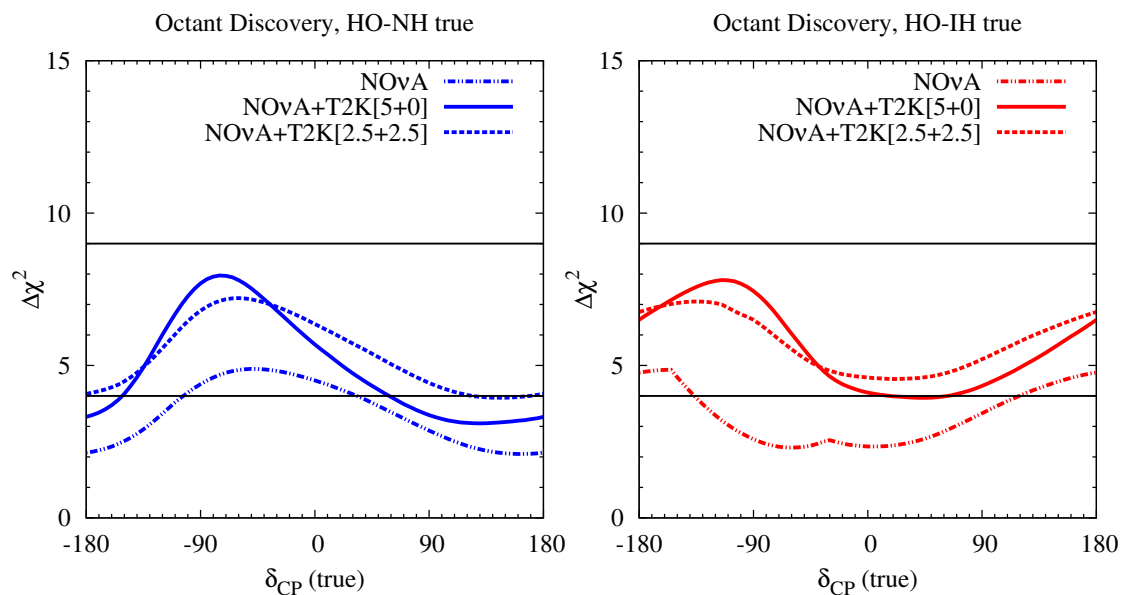


**Figure 11:** Octant resolving capability as a function of true  $\delta_{\text{CP}}$  for various set-ups . In these plots, HO is assumed to be the true octant. The left (right) panel corresponds to NH (IH) being the true hierarchy.

From figure 10, we see that the combined data from  $\text{NO}\nu\text{A}$  and T2K ( $5\nu$ ) give a  $2\sigma$  octant resolution for all values of true  $\delta_{\text{CP}}$  if LO is the true octant. From figure 11, we see that this combined data can rule out the wrong octant at  $2\sigma$  for HO-IH, but not for

HO-NH. The problem of HO-NH can be solved if the T2K has equal  $\nu$  and  $\bar{\nu}$  runs of 2.5 years each. This change improves the octant determination for the unfavorable values of true  $\delta_{\text{CP}}$  (where  $\Delta\chi^2$  is minimum) for all four combinations of hierarchy and octant. In particular, for the case of HO-NH, it leads to a complete ruling out of the wrong octant at  $2\sigma$  for all values of true  $\delta_{\text{CP}}$ . Thus, balanced runs of T2K in  $\nu - \bar{\nu}$  mode is preferred over a pure  $\nu$  run because of better octant determination capability.

Figures 10 and 11 show that the combined data from NO $\nu$ A and T2K has a better overall octant resolving capability if LO is the true octant. We found out that this feature of LO being more favorable compared to HO is a consequence of marginalization over the oscillation parameters (mainly  $\delta_{\text{CP}}$ ) and the systematic uncertainties. We checked that in the absence of any kind of marginalization  $\Delta\chi_{\text{HO}}^2$  is consistently larger than  $\Delta\chi_{\text{LO}}^2$ .

### 5.3 Octant resolution as function of true $\theta_{23}$

In the discussion so far, we assumed the true values of  $\sin^2 \theta_{23}$  to be 0.41 for LO and 0.59 for HO. These are, of course, the best-fit points from the global analyses. But, we must consider the octant resolution capability for values of true  $\sin^2 \theta_{23}$  in the full allowed range (0.34, 0.67). In this subsection, we calculate the octant resolution capability of NO $\nu$ A and T2K as a function of both true  $\sin^2 \theta_{23}$  and true  $\delta_{\text{CP}}$ . It was shown earlier that equal  $\nu - \bar{\nu}$  runs are superior to pure  $\nu$  run for octant resolution. Hence, in this subsection, the calculations are done only for the following run combination:  $(3\nu + 3\bar{\nu})$  for NO $\nu$ A and  $(2.5\nu + 2.5\bar{\nu})$  for T2K.

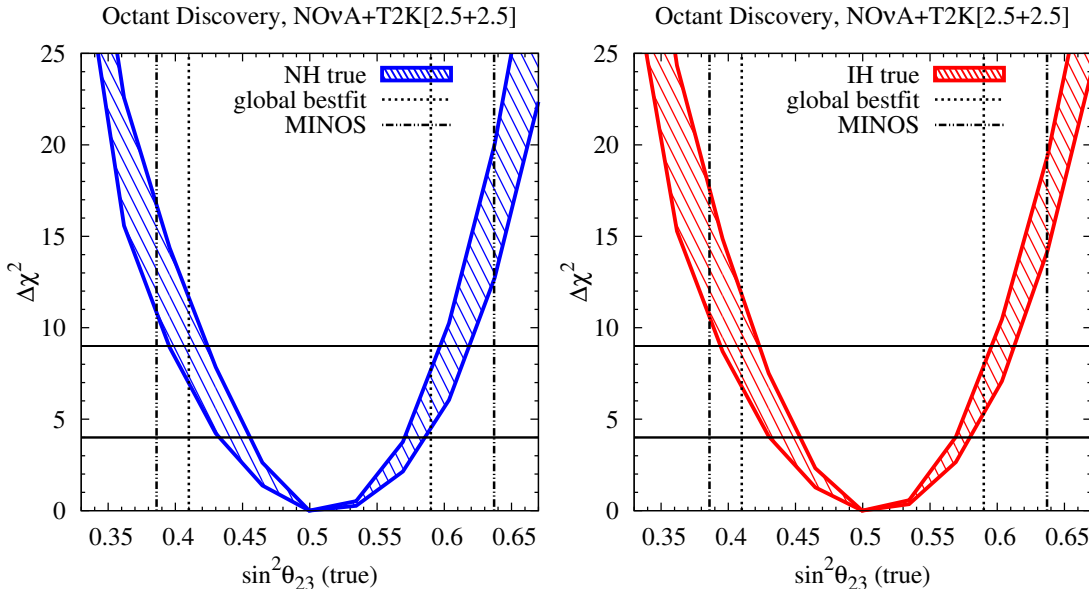


**Figure 12:** Octant resolving capability as a function of true  $\sin^2 \theta_{23}$  for the combined  $3\nu + 3\bar{\nu}$  runs of NO $\nu$ A and  $2.5\nu + 2.5\bar{\nu}$  runs of T2K. The variation in values of  $\Delta\chi^2$  for a given true  $\sin^2 \theta_{23}$  is due to the variation in true  $\delta_{\text{CP}}$ . The vertical lines correspond to the best-fit values of global data and those of MINOS accelerator data. The left (right) panel corresponds to NH (IH) being the true hierarchy.

In figure 12, we plotted the  $\Delta\chi^2$  vs. the true value of  $\sin^2\theta_{23}$ . This  $\Delta\chi^2$  is computed for the given true value of  $\sin^2\theta_{23}$  with true  $\delta_{\text{CP}}$  varying between  $(-180^\circ, 180^\circ)$ . This variation in  $\delta_{\text{CP}}$  leads to the band of values in  $\Delta\chi^2$ . As expected, the octant resolution is poor for true  $\sin^2\theta_{23}$  close to 0.5. A  $2\sigma$  octant resolution is possible for  $\sin^2\theta_{23} \leq 0.43$  and for  $\sin^2\theta_{23} \geq 0.58$ , for all values of  $\delta_{\text{CP}}$ . This is consistent with our earlier claim that  $2\sigma$  octant resolution is possible for the global best-fit values of  $\sin^2\theta_{23}$ .

As mentioned earlier, MINOS favors a non-maximal value of  $\sin^2 2\theta_{\text{eff}} = 0.94$ . This gives two degenerate solutions,  $\theta_{23} \approx 38^\circ$  ( $\sin^2\theta_{23} = 0.386$ ) in LO and  $\theta_{23} \approx 53^\circ$  ( $\sin^2\theta_{23} = 0.637$ ) in HO. Note that these values are not complementary because of the  $\theta_{13}$ -dependent correction described in equation 2.3. For these values, a better than  $3\sigma$  octant resolution is possible, which is true for both choices of true hierarchy.

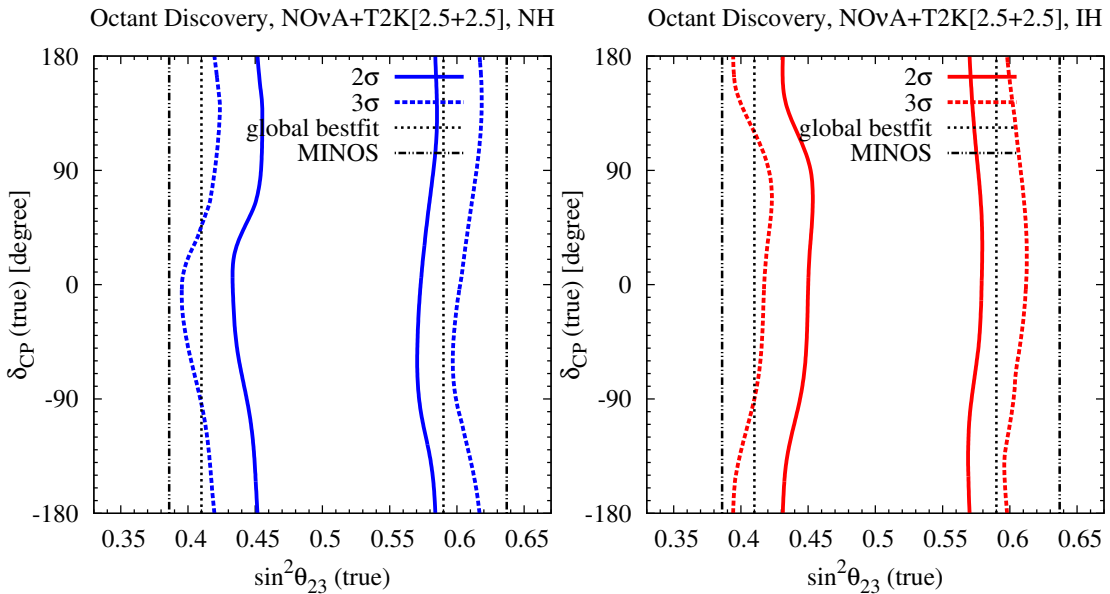


**Figure 13:** Octant resolving capability in the true  $\sin^2\theta_{23}$  - true  $\delta_{\text{CP}}$  plane for the combined  $3\nu + 3\bar{\nu}$  runs of NO $\nu$ A and  $2.5\nu + 2.5\bar{\nu}$  runs of T2K. Both  $2\sigma$  and  $3\sigma$  C.L. contours are plotted. The vertical lines correspond to the best-fit values of global data and those of MINOS accelerator data. The left (right) panel corresponds to NH (IH) being the true hierarchy.

In figure 13, we plotted the  $2\sigma$  and  $3\sigma$  octant resolution contours in true  $\sin^2\theta_{23}$  - true  $\delta_{\text{CP}}$  plane. Octant resolution is possible only for points lying outside the contours. These figures again show that octant resolution is possible at  $2\sigma$  for global best-fit points and at  $3\sigma$  for MINOS best-fit points. The results for the two hierarchies are similar here also.

## 6 Summary and Conclusions

Recently, the preliminary results from MINOS experiment have indicated that  $\theta_{23}$  is not maximal. This raises the question of the true octant of  $\theta_{23}$  *i.e.* whether  $\theta_{23} < 45^\circ$  (LO) or  $\theta_{23} > 45^\circ$  (HO).  $\nu_e$  appearance searches at the presently running T2K and upcoming

NO $\nu$ A experiments are sensitive to the octant, especially in light of moderately large  $\theta_{13}$ . The main difficulty in octant resolution stems from octant- $\delta_{\text{CP}}$  degeneracy. We explored this degeneracy in detail and found that equal neutrino and anti-neutrino runs are mandatory to overcome this problem. This is because the octant- $\delta_{\text{CP}}$  combinations, which have degenerate probabilities in the neutrino data are free of this degeneracy in the anti-neutrino data and vice-versa. We observe that equal  $\nu - \bar{\nu}$  runs for T2K and NO $\nu$ A overcome the octant- $\delta_{\text{CP}}$  degeneracy for both NH and IH. We also studied the prospects of T2K and NO $\nu$ A to improve the precision in  $\theta_{23}$ . The  $\nu_{\mu}$  disappearance data leads to two degenerate solutions of  $\sin^2 \theta_{23}$ , one in each octant. For  $\sin^2 \theta_{23} = 0.41$  (0.59), the expected precision will be  $\delta(\sin^2 \theta_{23}) = 0.015$  (0.02). The  $\nu_e$  appearance data can resolve the octant degeneracy for the best-fit values. NO $\nu$ A alone can rule out the wrong octant at  $2\sigma$  if  $\sin^2 \theta_{23} = 0.41$ , independently of hierarchy and  $\delta_{\text{CP}}$ . Combined data from equal neutrino and anti-neutrino runs of T2K (2.5 years each) and NO $\nu$ A (3 years each) can establish the correct octant at  $2\sigma$  C.L. for any combination of hierarchy and  $\delta_{\text{CP}}$ , if  $\sin^2 \theta_{23} \leq 0.43$  or  $\geq 0.58$ . A  $3\sigma$  discovery is possible if  $\sin^2 \theta_{23} \leq 0.39$  or  $\geq 0.62$  with the same set of runs.

## Acknowledgments

SKA would like to thank Pilar Hernández and Mariam Tortola for useful discussions. SKA acknowledges the support from the Spanish Ministry for Education and Science projects FPA2007-60323 and FPA2011-29678; the Consolider-Ingenio CUP (CSD2008-00037) and CPAN (CSC2007-00042); the Generalitat Valenciana (PROMETEO/2009/116); the European projects LAGUNA (Project Number 212343) and the ITN INVISIBLES (Marie Curie Actions, PITN- GA-2011-289442).

## A Events vs. $\delta_{\text{CP}}$

In this appendix, we consider the variation of appearance events as a function of  $\delta_{\text{CP}}$  in both  $\nu$  and  $\bar{\nu}$  modes.

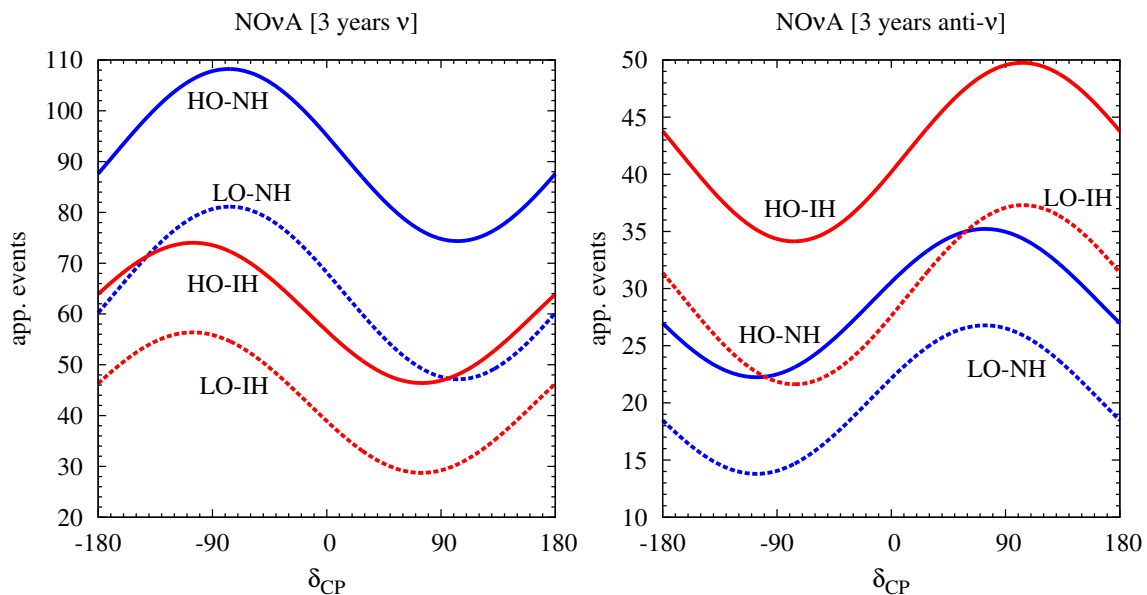


**Figure 14:** Total appearance events rates for all possible combinations of octant and hierarchy as a function of the  $\delta_{CP}$ . The left (right) panel is for  $\nu$  ( $\bar{\nu}$ ) running. These plots are for NO $\nu$ A (L=810 km),  $\sin^2 2\theta_{13} = 0.089$ . For LO (HO),  $\sin^2 \theta_{23} = 0.41$  (0.59).

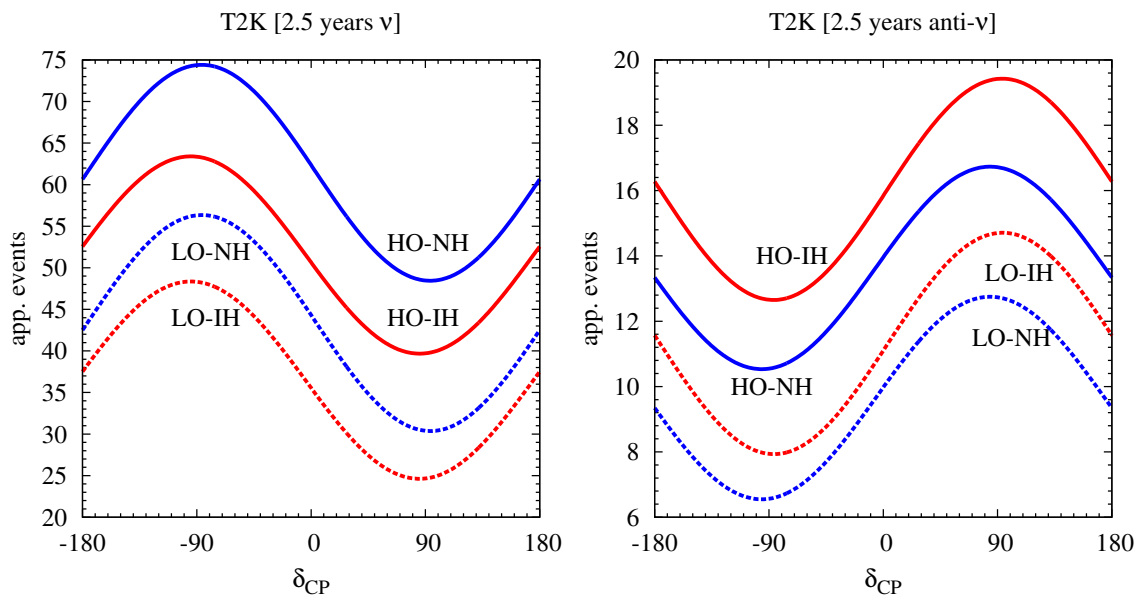


**Figure 15:** Total appearance events rates for all possible combinations of octant and hierarchy as a function of the  $\delta_{CP}$ . The left (right) panel is for  $\nu$  ( $\bar{\nu}$ ) running. These plots are for T2K (L=295 km),  $\sin^2 2\theta_{13} = 0.089$ . For LO (HO),  $\sin^2 \theta_{23} = 0.41$  (0.59).

In figure 14, we show the variation of  $\nu_{\mu} \rightarrow \nu_e$  appearance events vs.  $\delta_{CP}$  for NO $\nu$ A in

both  $\nu$  and  $\bar{\nu}$  modes. We see from the left panel ( $\nu$  events) that the combinations HO-NH and LO-IH are well separated but the other two combinations- HO-IH and LO-NH have essentially the same event numbers. But in the right panel ( $\bar{\nu}$  events), HO-IH and LO-NH are well separated and the other two combinations are nearly degenerate. Thus, we see that the unfavorable combinations in  $\nu$  mode are favorable in  $\bar{\nu}$  mode and vice-versa. This feature is seen in the event rates for T2K also as shown in figure 15 where we have assumed T2K to have 2.5 years of each neutrino and anti-neutrino run .

## B Allowed regions in test $\delta_{\text{CP}}$ - test $\sin^2 \theta_{23}$ plane

In section 3, we saw that the CP conserving values of  $\delta_{\text{CP}}$  pose the biggest challenge in octant determination. Therefore, in this appendix, we simulate T2K and NO $\nu$ A data for true  $\delta_{\text{CP}} = 0$  and analyze it. Figures 16-19 are drawn for each of the four possible combinations of true hierarchy and true octant. These figures show the regions allowed by the data in the test  $\delta_{\text{CP}}$  - test  $\sin^2 \theta_{23}$  plane at  $2\sigma$  ( $\Delta\chi^2 \leq 6.18$  for 2 d.o.f.).

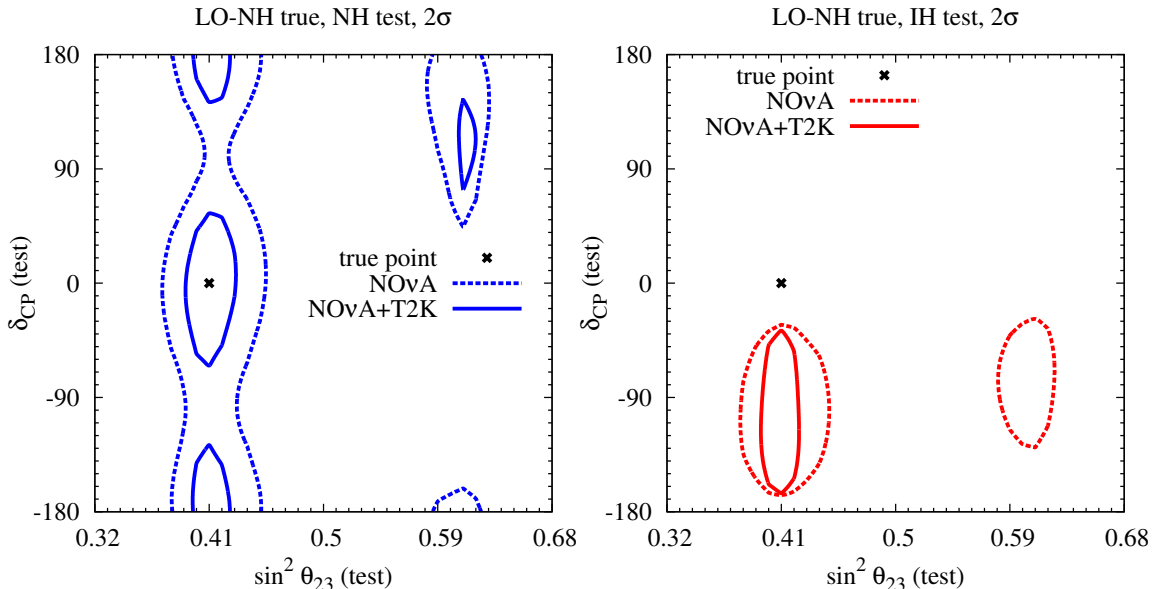


**Figure 16:** Allowed regions in test  $\delta_{\text{CP}}$  - test  $\sin^2 \theta_{23}$  plane at  $2\sigma$  (2 d.o.f.) C.L. for true  $\delta_{\text{CP}} = 0$ . LO-NH is assumed to be the true combination. The left (right) panel corresponds to NH (IH) being the test hierarchy.

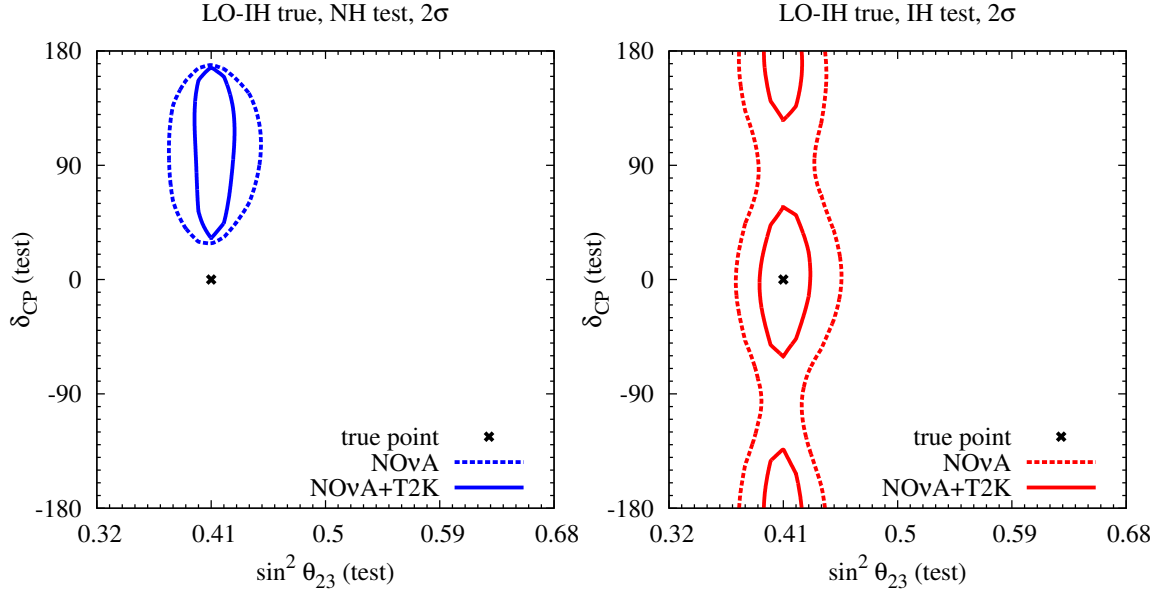


**Figure 17:** Allowed regions in test  $\delta_{\text{CP}}$  - test  $\sin^2 \theta_{23}$  plane at  $2\sigma$  (2 d.o.f.) C.L. for true  $\delta_{\text{CP}} = 0$ . LO-IH is assumed to be the true combination. The left (right) panel corresponds to NH (IH) being the test hierarchy.

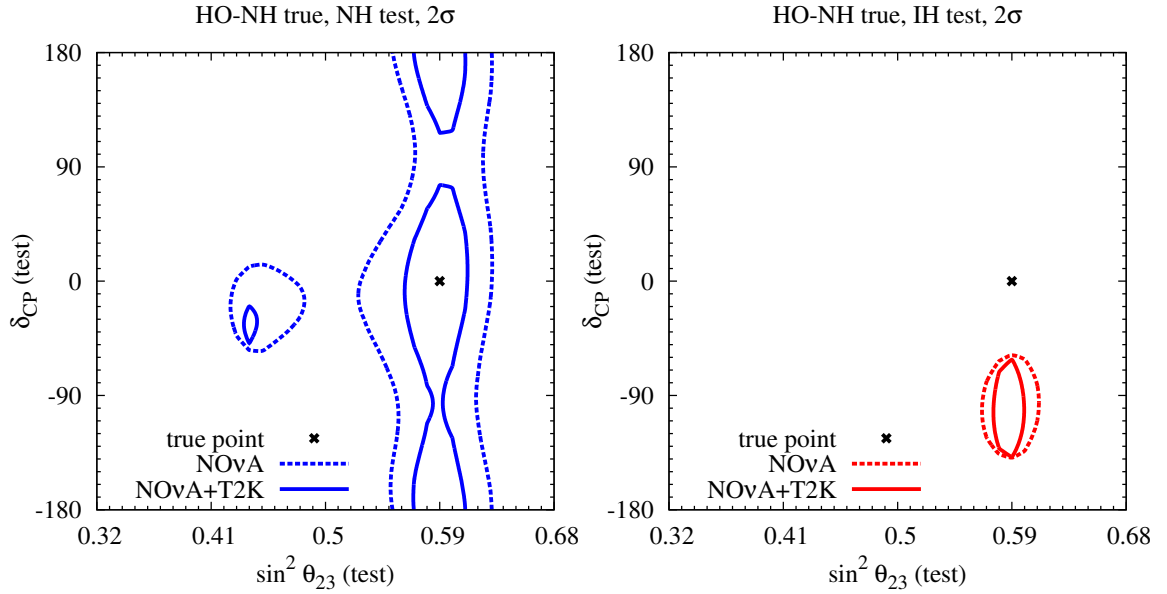


**Figure 18:** Allowed regions in test  $\delta_{\text{CP}}$  - test  $\sin^2 \theta_{23}$  plane at  $2\sigma$  (2 d.o.f.) C.L. for true  $\delta_{\text{CP}} = 0$ . HO-NH is assumed to be the true combination. The left (right) panel corresponds to NH (IH) being the test hierarchy.



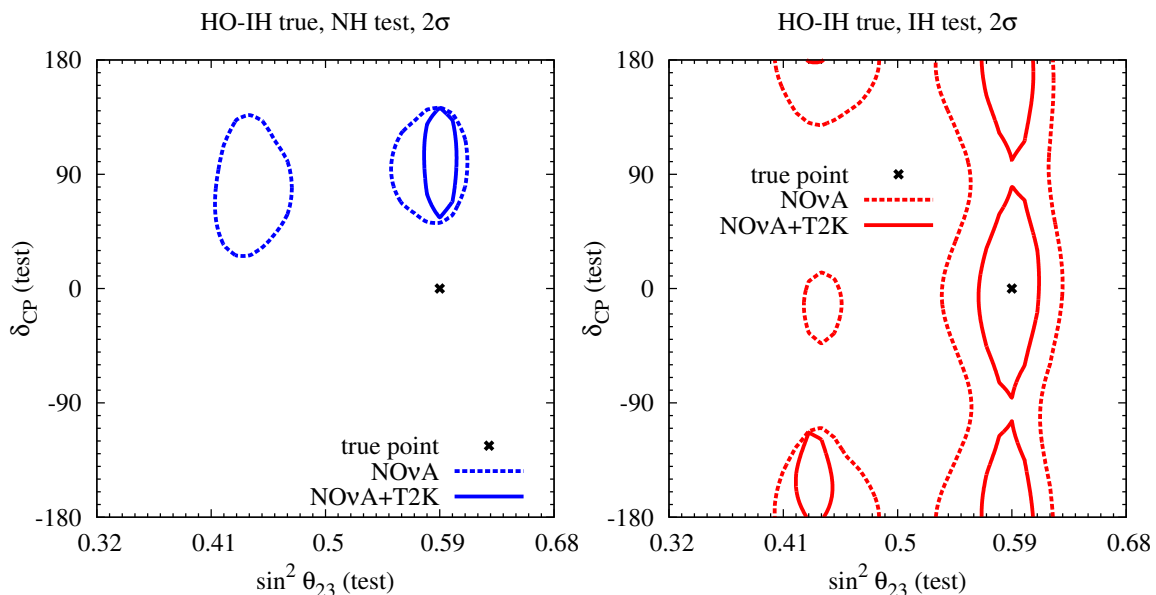


**Figure 19:** Allowed regions in test  $\delta_{CP}$  - test  $\sin^2 \theta_{23}$  plane at  $2\sigma$  (2 d.o.f.) C.L. for true  $\delta_{CP} = 0$ . HO-IH is assumed to be the true combination. The left (right) panel corresponds to NH (IH) being the test hierarchy.

These figures illustrate that, in general, the combined data of T2K and NO $\nu$ A discriminate against the wrong octant of  $\theta_{23}$ . Also, note that, these figures give us the allowed ranges in both  $\sin^2 \theta_{23}$  and  $\delta_{CP}$  (2 d.o.f.) around the right and wrong octant for the single value of true  $\delta_{CP} = 0$ .

## References

- [1] **DAYA-BAY** Collaboration, F. An et al., *Observation of electron-antineutrino disappearance at Daya Bay*, *Phys.Rev.Lett.* **108** (2012) 171803, [[arXiv:1203.1669](https://arxiv.org/abs/1203.1669)].
- [2] **RENO** Collaboration, J. Ahn et al., *Observation of Reactor Electron Antineutrino Disappearance in the RENO Experiment*, *Phys.Rev.Lett.* **108** (2012) 191802, [[arXiv:1204.0626](https://arxiv.org/abs/1204.0626)].
- [3] **DAYA-BAY** Collaboration, D. Dwyer, *Improved measurement of electron- $\bar{\nu}$  disappearance at daya bay*, 2012. Talk given at the Neutrino 2012 Conference, June 3-9, 2012, Kyoto, Japan, <http://neu2012.kek.jp/>.
- [4] **RENO** Collaboration, S. Kim, *Observation of reactor antineutrino disappearance at reno*, 2012. Talk given at the Neutrino 2012 Conference, June 3-9, 2012, Kyoto, Japan, <http://neu2012.kek.jp/>.
- [5] **T2K** Collaboration, K. Abe et al., *Indication of Electron Neutrino Appearance from an Accelerator-produced Off-axis Muon Neutrino Beam*, *Phys.Rev.Lett.* **107** (2011) 041801, [[arXiv:1106.2822](https://arxiv.org/abs/1106.2822)].
- [6] **T2K** Collaboration, T. Nakaya, *New results from t2k*, 2012. Talk given at the Neutrino 2012 Conference, June 3-9, 2012, Kyoto, Japan, <http://neu2012.kek.jp/>.

- [7] **MINOS** Collaboration, P. Adamson et al., *Improved search for muon-neutrino to electron-neutrino oscillations in MINOS*, *Phys.Rev.Lett.* **107** (2011) 181802, [[arXiv:1108.0015](#)].
- [8] **MINOS** Collaboration, R. Nichol, *Final MINOS Results*, 2012. Talk given at the Neutrino 2012 Conference, June 3-9, 2012, Kyoto, Japan, <http://neu2012.kek.jp/>.
- [9] **Double Chooz** Collaboration, Y. Abe et al., *Indication for the disappearance of reactor electron antineutrinos in the Double Chooz experiment*, *Phys.Rev.Lett.* **108** (2012) 131801, [[arXiv:1112.6353](#)].
- [10] **Double Chooz** Collaboration, Y. Abe et al., *Reactor electron antineutrino disappearance in the Double Chooz experiment*, [arXiv:1207.6632](#).
- [11] D. Forero, M. Tortola, and J. Valle, *Global status of neutrino oscillation parameters after Neutrino-2012*, *Phys.Rev.* **D86** (2012) 073012, [[arXiv:1205.4018](#)].
- [12] G. Fogli, E. Lisi, A. Marrone, D. Montanino, A. Palazzo, et al., *Global analysis of neutrino masses, mixings and phases: entering the era of leptonic CP violation searches*, *Phys.Rev.* **D86** (2012) 013012, [[arXiv:1205.5254](#)].
- [13] M. Gonzalez-Garcia, M. Maltoni, J. Salvado, and T. Schwetz, *Global fit to three neutrino mixing: critical look at present precision*, [arXiv:1209.3023](#).
- [14] J. Hewett, H. Weerts, R. Brock, J. Butler, B. Casey, et al., *Fundamental Physics at the Intensity Frontier*, [arXiv:1205.2671](#).
- [15] H. Minakata, *Phenomenology of future neutrino experiments with large  $\theta(13)$* , 2012. Talk given at the Neutrino 2012 Conference, June 3-9, 2012, Kyoto, Japan, <http://neu2012.kek.jp/>.
- [16] Y. Itow, *Atmospheric neutrinos: Results from running experiments*, 2012. Talk given at the Neutrino 2012 Conference, June 3-9, 2012, Kyoto, Japan, <http://neu2012.kek.jp/>.
- [17] R. Mohapatra and A. Smirnov, *Neutrino Mass and New Physics*, *Ann.Rev.Nucl.Part.Sci.* **56** (2006) 569–628, [[hep-ph/0603118](#)].
- [18] C. H. Albright and M.-C. Chen, *Model Predictions for Neutrino Oscillation Parameters*, *Phys.Rev.* **D74** (2006) 113006, [[hep-ph/0608137](#)].
- [19] C. H. Albright, A. Dueck, and W. Rodejohann, *Possible Alternatives to Tri-bimaximal Mixing*, *Eur.Phys.J.* **C70** (2010) 1099–1110, [[arXiv:1004.2798](#)].
- [20] S. F. King and C. Luhn, *Neutrino Mass and Mixing with Discrete Symmetry*, [arXiv:1301.1340](#).
- [21] T. Fukuyama and H. Nishiura, *Mass matrix of Majorana neutrinos*, [hep-ph/9702253](#).
- [22] R. N. Mohapatra and S. Nussinov, *Bimaximal neutrino mixing and neutrino mass matrix*, *Phys.Rev.* **D60** (1999) 013002, [[hep-ph/9809415](#)].
- [23] C. Lam, *A 2-3 symmetry in neutrino oscillations*, *Phys.Lett.* **B507** (2001) 214–218, [[hep-ph/0104116](#)].
- [24] P. Harrison and W. Scott,  *$\mu$  -  $\tau$  reflection symmetry in lepton mixing and neutrino oscillations*, *Phys.Lett.* **B547** (2002) 219–228, [[hep-ph/0210197](#)].
- [25] T. Kitabayashi and M. Yasue,  *$S(2L)$  permutation symmetry for left-handed  $\mu$  and  $\tau$  families and neutrino oscillations in an  $SU(3)$ - $L \times SU(1)$ - $N$  gauge model*, *Phys.Rev.* **D67** (2003) 015006, [[hep-ph/0209294](#)].

- [26] W. Grimus and L. Lavoura, *A Discrete symmetry group for maximal atmospheric neutrino mixing*, *Phys.Lett.* **B572** (2003) 189–195, [[hep-ph/0305046](#)].
- [27] A. Ghosal, *An  $SU(2)(L) \times U(1)(Y)$  model with reflection symmetry in view of recent neutrino experimental result*, [hep-ph/0304090](#).
- [28] Y. Koide, *Universal texture of quark and lepton mass matrices with an extended flavor  $2\text{-}\hat{3}$  symmetry*, *Phys.Rev.* **D69** (2004) 093001, [[hep-ph/0312207](#)].
- [29] R. Mohapatra and W. Rodejohann, *Broken mu-tau symmetry and leptonic CP violation*, *Phys.Rev.* **D72** (2005) 053001, [[hep-ph/0507312](#)].
- [30] E. Ma, *Plato's fire and the neutrino mass matrix*, *Mod.Phys.Lett.* **A17** (2002) 2361–2370, [[hep-ph/0211393](#)].
- [31] E. Ma and G. Rajasekaran, *Softly broken  $A(4)$  symmetry for nearly degenerate neutrino masses*, *Phys.Rev.* **D64** (2001) 113012, [[hep-ph/0106291](#)].
- [32] K. Babu, E. Ma, and J. Valle, *Underlying  $A(4)$  symmetry for the neutrino mass matrix and the quark mixing matrix*, *Phys.Lett.* **B552** (2003) 207–213, [[hep-ph/0206292](#)].
- [33] W. Grimus and L. Lavoura,  *$S(3) \times Z(2)$  model for neutrino mass matrices*, *JHEP* **0508** (2005) 013, [[hep-ph/0504153](#)].
- [34] E. Ma, *Tetrahedral family symmetry and the neutrino mixing matrix*, *Mod.Phys.Lett.* **A20** (2005) 2601–2606, [[hep-ph/0508099](#)].
- [35] M. Raidal, *Relation between the neutrino and quark mixing angles and grand unification*, *Phys.Rev.Lett.* **93** (2004) 161801, [[hep-ph/0404046](#)].
- [36] H. Minakata and A. Y. Smirnov, *Neutrino mixing and quark-lepton complementarity*, *Phys.Rev.* **D70** (2004) 073009, [[hep-ph/0405088](#)].
- [37] J. Ferrandis and S. Pakvasa, *Quark-lepton complementarity relation and neutrino mass hierarchy*, *Phys.Rev.* **D71** (2005) 033004, [[hep-ph/0412038](#)].
- [38] S. Antusch, S. F. King, and R. N. Mohapatra, *Quark-lepton complementarity in unified theories*, *Phys.Lett.* **B618** (2005) 150–161, [[hep-ph/0504007](#)].
- [39] G. L. Fogli and E. Lisi, *Tests of three flavor mixing in long baseline neutrino oscillation experiments*, *Phys.Rev.* **D54** (1996) 3667–3670, [[hep-ph/9604415](#)].
- [40] V. Barger, D. Marfatia, and K. Whisnant, *Breaking eight fold degeneracies in neutrino CP violation, mixing, and mass hierarchy*, *Phys.Rev.* **D65** (2002) 073023, [[hep-ph/0112119](#)].
- [41] H. Minakata, H. Nunokawa, and S. J. Parke, *Parameter degeneracies in neutrino oscillation measurement of leptonic CP and T violation*, *Phys.Rev.* **D66** (2002) 093012, [[hep-ph/0208163](#)].
- [42] J. Burguet-Castell, M. Gavela, J. Gomez-Cadenas, P. Hernandez, and O. Mena, *On the Measurement of leptonic CP violation*, *Nucl.Phys.* **B608** (2001) 301–318, [[hep-ph/0103258](#)].
- [43] H. Minakata and H. Nunokawa, *Exploring neutrino mixing with low-energy superbeams*, *JHEP* **0110** (2001) 001, [[hep-ph/0108085](#)].
- [44] H. Minakata, H. Sugiyama, O. Yasuda, K. Inoue, and F. Suekane, *Reactor measurement of  $\theta(13)$  and its complementarity to long baseline experiments*, *Phys.Rev.* **D68** (2003) 033017, [[hep-ph/0211111](#)].

- [45] K. Hiraide, H. Minakata, T. Nakaya, H. Nunokawa, H. Sugiyama, et al., *Resolving  $\theta_{23}$  degeneracy by accelerator and reactor neutrino oscillation experiments*, *Phys.Rev.* **D73** (2006) 093008, [[hep-ph/0601258](#)].
- [46] A. Donini, D. Meloni, and P. Migliozzi, *The Silver channel at the neutrino factory*, *Nucl.Phys.* **B646** (2002) 321–349, [[hep-ph/0206034](#)].
- [47] D. Meloni, *Solving the octant degeneracy with the Silver channel*, *Phys.Lett.* **B664** (2008) 279–284, [[arXiv:0802.0086](#)].
- [48] S. Antusch, P. Huber, J. Kersten, T. Schwetz, and W. Winter, *Is there maximal mixing in the lepton sector?*, *Phys.Rev.* **D70** (2004) 097302, [[hep-ph/0404268](#)].
- [49] H. Minakata, M. Sonoyama, and H. Sugiyama, *Determination of  $\theta_{23}$  in long-baseline neutrino oscillation experiments with three-flavor mixing effects*, *Phys.Rev.* **D70** (2004) 113012, [[hep-ph/0406073](#)].
- [50] M. Gonzalez-Garcia, M. Maltoni, and A. Y. Smirnov, *Measuring the deviation of the 2-3 lepton mixing from maximal with atmospheric neutrinos*, *Phys.Rev.* **D70** (2004) 093005, [[hep-ph/0408170](#)].
- [51] D. Choudhury and A. Datta, *Detecting matter effects in long baseline experiments*, *JHEP* **0507** (2005) 058, [[hep-ph/0410266](#)].
- [52] S. Choubey and P. Roy, *Probing the deviation from maximal mixing of atmospheric neutrinos*, *Phys.Rev.* **D73** (2006) 013006, [[hep-ph/0509197](#)].
- [53] D. Indumathi, M. Murthy, G. Rajasekaran, and N. Sinha, *Neutrino oscillation probabilities: Sensitivity to parameters*, *Phys.Rev.* **D74** (2006) 053004, [[hep-ph/0603264](#)].
- [54] T. Kajita, H. Minakata, S. Nakayama, and H. Nunokawa, *Resolving eight-fold neutrino parameter degeneracy by two identical detectors with different baselines*, *Phys.Rev.* **D75** (2007) 013006, [[hep-ph/0609286](#)].
- [55] K. Hagiwara and N. Okamura, *Solving the degeneracy of the lepton-flavor mixing angle  $\theta_{ATM}$  by the T2KK two detector neutrino oscillation experiment*, *JHEP* **0801** (2008) 022, [[hep-ph/0611058](#)].
- [56] A. Samanta and A. Y. Smirnov, *The 2-3 mixing and mass split: atmospheric neutrinos and magnetized spectrometers*, *JHEP* **1107** (2011) 048, [[arXiv:1012.0360](#)].
- [57] **T2K** Collaboration, Y. Itow et al., *The JHF-Kamioka neutrino project*, [hep-ex/0106019](#).
- [58] **NOvA** Collaboration, D. Ayres et al., *NOvA: Proposal to build a 30 kiloton off-axis detector to study  $\nu(\mu)$  to  $\nu(e)$  oscillations in the NuMI beamline*, [hep-ex/0503053](#).
- [59] **NOvA** Collaboration, R. Patterson, *The NOvA Experiment: Status and Outlook*, 2012. Talk given at the Neutrino 2012 Conference, June 3-9, 2012, Kyoto, Japan, <http://neu2012.kek.jp/>.
- [60] H. Nunokawa, S. J. Parke, and R. Zukanovich Funchal, *Another possible way to determine the neutrino mass hierarchy*, *Phys.Rev.* **D72** (2005) 013009, [[hep-ph/0503283](#)].
- [61] A. de Gouvea, J. Jenkins, and B. Kayser, *Neutrino mass hierarchy, vacuum oscillations, and vanishing  $U(e3)$* , *Phys.Rev.* **D71** (2005) 113009, [[hep-ph/0503079](#)].
- [62] S. K. Raut, *Effect of non-zero  $\theta_{13}$  on the measurement of  $\theta_{23}$* , [arXiv:1209.5658](#).
- [63] **Particle Data Group** Collaboration, J. Beringer et al., *Review of Particle Physics (RPP)*, *Phys.Rev.* **D86** (2012) 010001.

- [64] E. K. Akhmedov, R. Johansson, M. Lindner, T. Ohlsson, and T. Schwetz, *Series expansions for three flavor neutrino oscillation probabilities in matter*, *JHEP* **0404** (2004) 078, [[hep-ph/0402175](#)].
- [65] A. Cervera, A. Donini, M. Gavela, J. Gomez Cadenas, P. Hernandez, et al., *Golden measurements at a neutrino factory*, *Nucl.Phys.* **B579** (2000) 17–55, [[hep-ph/0002108](#)].
- [66] M. Freund, *Analytic approximations for three neutrino oscillation parameters and probabilities in matter*, *Phys.Rev.* **D64** (2001) 053003, [[hep-ph/0103300](#)].
- [67] L. Wolfenstein, *Neutrino oscillations in matter*, *Phys. Rev.* **D17** (1978) 2369–2374.
- [68] O. Mena and S. J. Parke, *Untangling CP violation and the mass hierarchy in long baseline experiments*, *Phys.Rev.* **D70** (2004) 093011, [[hep-ph/0408070](#)].
- [69] S. Prakash, S. K. Raut, and S. U. Sankar, *Getting the Best Out of T2K and NOvA*, *Phys.Rev.* **D86** (2012) 033012, [[arXiv:1201.6485](#)].
- [70] P. Huber, M. Lindner, and W. Winter, *Simulation of long-baseline neutrino oscillation experiments with GLoBES (General Long Baseline Experiment Simulator)*, *Comput.Phys.Commun.* **167** (2005) 195, [[hep-ph/0407333](#)].
- [71] P. Huber, J. Kopp, M. Lindner, M. Rolinec, and W. Winter, *New features in the simulation of neutrino oscillation experiments with GLoBES 3.0: General Long Baseline Experiment Simulator*, *Comput.Phys.Commun.* **177** (2007) 432–438, [[hep-ph/0701187](#)].
- [72] P. Huber, M. Lindner, T. Schwetz, and W. Winter, *First hint for CP violation in neutrino oscillations from upcoming superbeam and reactor experiments*, *JHEP* **0911** (2009) 044, [[arXiv:0907.1896](#)].
- [73] M. Fechner, *Détermination des performances attendues sur la recherche de l’oscillation  $\nu_{\mu} \rightarrow \nu_{\tau}$  to nue dans l’expérience T2K depuis l’étude des données recueillies dans l’expérience K2K*, . Presented on 9 May 2006.
- [74] **NOvA** Collaboration, D. Ayres et al., *The NOvA Technical Design Report*, tech. rep., 2007. FERMILAB-DESIGN-2007-01.
- [75] S. K. Agarwalla, S. Prakash, S. K. Raut, and S. U. Sankar, *Potential of optimized NOvA for large  $\theta_{13}$  & combined performance with a LArTPC & T2K*, *JHEP* **1212** (2012) 075, [[arXiv:1208.3644](#)].
- [76] **Daya Bay** Collaboration, X. Qian, *Improved Measurement of Electron-antineutrino Disappearance at Daya Bay*, 2012. Talk given at the NuFact 2012 Conference, July 23-28, 2012, Williamsburg, USA, <http://www.jlab.org/conferences/nufact12/>.